

Quantum Stabilizer Codes for Correlated and Asymmetric Depolarizing Errors

Carlo Cafaro¹ and Stefano Mancini²

^{1,2}*School of Science and Technology, Physics Division,
University of Camerino, I-62032 Camerino, Italy*

We study the performance of common quantum stabilizer codes in the presence of asymmetric and correlated errors. Specifically, we consider the depolarizing noisy quantum memory channel and perform quantum error correction via the five and seven-qubit stabilizer codes. We characterize these codes by means of the entanglement fidelity as function of the error probability and the degree of memory. We show that their performances are lowered by the presence of correlations and we compute the error probability threshold values for codes effectiveness. Furthermore, we uncover that the asymmetry in the error probabilities does not affect the performance of the five-qubit code while it does affect the performance of the seven-qubit code which results less effective when considering correlated and symmetric depolarizing errors but more effective for correlated and asymmetric errors.

PACS numbers: quantum error correction (03.67.Pp); decoherence (03.65. Yz).

I. INTRODUCTION

The most important obstacle in quantum information processing is decoherence. It causes a quantum computer to lose its quantum properties destroying its performance advantages over a classical computer. The unavoidable interaction between the open quantum processor and its environment corrupts the information stored in the system and causes errors that may lead to wrong outputs. In general, environments may be very complex systems characterized by many uncontrollable degrees of freedom. A useful active strategy to defend quantum coherence of a processing against environmental noise is that of quantum error correcting codes (QECC) [1–3] where, in analogy to classical information theory, quantum information is stabilized by using redundant encoding and measurements.

The formal mathematical description of the qubit-environment interaction is often given in terms of quantum channels. Quantum error correction is usually developed under the assumption of i.i.d. (identically and independently distributed) errors. These error models are characterized by memoryless communication channels Λ such that n -channel uses is given by $\Lambda^{(n)} = \Lambda^{\otimes n}$. In such cases of complete independent decoherence, qubits interact with their own environments which do not interact with each other. However, in actual physical situations, qubits may interact with a common environment which unavoidably introduces correlations in the noise. For instance, there are situations where qubits in a ion trap set-up are collectively coupled to their vibrational modes [4]. In other situations, different qubits in a quantum dot design are coupled to the same lattice, thus interacting with a common thermal bath of phonons [5]. The exchange of bosons between qubits causes spatial and temporal correlations that violate the condition of error independence [6]. Memory effects introduce correlations among channel uses with the consequence that $\Lambda^{(n)} \neq \Lambda^{\otimes n}$. Recent studies try to characterize the effect of correlations on the performance of QECCs [7–11]. It appears that correlations may have negative [8] or positive [9] impact on QECCs depending on the features of the error model being considered.

Furthermore, the noise may be asymmetric. Most of the quantum computing devices [12] are characterized by relaxation times ($\tau_{\text{relaxation}}$) that are one-two orders of magnitude larger than the corresponding dephasing times ($\tau_{\text{dephasing}}$). Relaxation leads to both bit-flip and phase-flip errors, whereas dephasing (loss of phase coherence, phase-shifting) only leads to phase-flip errors. Such asymmetry between $\tau_{\text{relaxation}}$ and $\tau_{\text{dephasing}}$ translates to an asymmetry in the occurrence probability of bit-flip (p_X) and phase-flip errors (p_Z). The ratio $\frac{p_Z}{p_X}$ is known as the channel asymmetry. Quantum error correction schemes should be designed in such a way that no resources (time and qubits) are wasted in attempting to detect and correct errors that may be relatively unlikely to occur. Quantum codes should be designed in order to exploit this asymmetry and provide better performance by neglecting the correction of less probable errors [13–15]. Indeed, examples of efficient quantum error-correcting codes (for instance, asymmetric stabilizer CSS codes) taking advantage of this asymmetry are given by families of codes of the Calderbank-Shor-Steane (CSS) type [16, 17].

Following these lines of investigations, in this article we study the performance of common quantum stabilizer codes in the presence of asymmetric and correlated errors. Specifically, we consider the depolarizing noisy quantum memory channel and perform quantum error correction via the five and seven-qubit stabilizer codes [18]. We characterize the performance of the codes by means of the entanglement fidelity $\mathcal{F}(\mu, p)$ [19] as function of the error probability p and degree of memory μ (correlations). We show that the performance of both codes is lowered in the presence of correlations and error probability threshold values for code effectiveness are computed vs. the degree of memory μ . The error correction schemes here considered only work for low values of μ . Furthermore, we uncover that the asymmetry

in the error probabilities does not affect the performance of the five-qubit code while it does affect the performance of the seven-qubit code which results less effective when considering correlated and symmetric depolarizing errors, but more effective for correlated and asymmetric errors.

The layout of the paper is as follows. In Section II, we consider a depolarizing noisy quantum memory channel characterized by symmetric error probabilities and QEC is performed via the $[[5, 1, 3]]$ stabilizer code. The performance of quantum error correcting codes is quantified by means of the entanglement fidelity $\mathcal{F}^{[[5,1,3]]}(\mu, p)$ as function of the error probability p and degree of memory μ . In Section III, QEC is performed via the $[[7, 1, 3]]$ -CSS stabilizer code. The performance of quantum error correcting codes is quantified by means of the entanglement fidelities $\mathcal{F}_{\text{Set-1}}^{[[7,1,3]]}(\mu, p)$ and $\mathcal{F}_{\text{Set-2}}^{[[7,1,3]]}(\mu, p)$ as function of the error probability p and degree of memory μ evaluated for two different allowable sets of correctable error operators. In Section IV, for asymmetric error probabilities and correlated noise errors, we show that the seven-qubit code can outperform the five qubit-code and it also endowed with a better threshold curve $\mu_{\text{threshold}} = \mu_{\text{threshold}}(p)$ where error correction is performed in an effective way. Finally, in Section V we present our final remarks.

II. THE FIVE-QUBIT CODE: SYMMETRIC ERROR PROBABILITIES AND CORRELATIONS

In this Section, we consider a depolarizing noisy quantum memory channel with symmetric error probabilities and QEC is performed via the $[[5, 1, 3]]$ stabilizer code. The performance of quantum error correcting codes is quantified by means of the entanglement fidelity $\mathcal{F}^{[[5,1,3]]}(\mu, p)$ as function of the error probability p and degree of memory μ .

Error Model. The depolarizing channel is especially easy to analyze in the context of quantum error-correction because it has a simple interpretation in terms of the four basic errors I, X, Y, Z which are the most commonly used in the analysis of quantum codes. However, this error model is rather general since the ability to error-correct the depolarizing channel automatically implies the ability to error-correct an arbitrary single qubit quantum operation. To simplify the notation, we may choose to omit sometimes the symbol of tensor product " \otimes " in the expressions for the error operators of weight greater than one.

Consider five qubits and Markov correlated errors in a depolarizing quantum channel $\Lambda^{(5)}(\rho)$,

$$\Lambda^{(5)}(\rho) = \sum_{i_1, i_2, i_3, i_4, i_5=0}^3 p_{i_5|i_4} p_{i_4|i_3} p_{i_3|i_2} p_{i_2|i_1} p_{i_1} \left[A_{i_5} A_{i_4} A_{i_3} A_{i_2} A_{i_1} \rho A_{i_1}^\dagger A_{i_2}^\dagger A_{i_3}^\dagger A_{i_4}^\dagger A_{i_5}^\dagger \right], \quad (1)$$

where $A_0 \equiv I, A_1 \equiv X, A_2 \equiv Y, A_3 \equiv Z$ are the Pauli operators defined as,

$$I|q\rangle \stackrel{\text{def}}{=} |q\rangle, X|q\rangle \stackrel{\text{def}}{=} |q \oplus 1\rangle, Z|q\rangle \stackrel{\text{def}}{=} (-1)^q |q\rangle, Y|q\rangle \stackrel{\text{def}}{=} i(-1)^q |q \oplus 1\rangle, \quad (2)$$

with $q = 0, 1$ and X, Y and Z given by,

$$X = \begin{pmatrix} 0 & 1 \\ 1 & 0 \end{pmatrix}, Y = iXZ = \begin{pmatrix} 0 & -i \\ i & 0 \end{pmatrix}, Z = \begin{pmatrix} 1 & 0 \\ 0 & -1 \end{pmatrix}. \quad (3)$$

The coefficients $p_{i_l|i_m}$ (conditional probabilities) with $l, m \in \{0, 1, \dots, 5\}$ satisfy the normalization condition,

$$\sum_{i_1, i_2, i_3, i_4, i_5=0}^3 p_{i_5|i_4} p_{i_4|i_3} p_{i_3|i_2} p_{i_2|i_1} p_{i_1} = 1. \quad (4)$$

For the depolarizing channel $\Lambda^{(5)}(\rho)$, coefficients $p_{i_l|i_m}$ are considered as,

$$p_{k|j} \stackrel{\text{def}}{=} (1 - \mu)p_k + \mu\delta_{k,j}, \quad p_{k=0} = 1 - p, p_{k=1, 2, 3} = p/3, \quad (5)$$

where $p \in [0, 1]$ denotes the error probability, $\mu \in [0, 1]$ represents the degree of memory ($\mu = 0$ gives the uncorrelated errors and $\mu = 1$ gives perfectly correlated errors) and $p_{k|j}$ is the probability of error k on qubit j . To simplify the notation, we may choose to suppress the bar " $|$ " appearing in the conditional probabilities ($p_{k|j} \equiv p_{k,j}$). Furthermore, since we are initially assuming $p_1 = p_2 = p_3 = p/3$, we are in the case of symmetric error probabilities.

Error Operators. In an explicit way, the depolarizing channel $\Lambda^{(5)}(\rho)$ can be written as,

$$\Lambda^{(5)}(\rho) = \sum_{k=0}^{2^{10}-1} A'_k \rho A_k^\dagger, \quad (6)$$

where A'_k are the enlarged error operators acting on the five qubit quantum states. The cardinality of the error operators defining $\Lambda^{(5)}(\rho)$ is 2^{10} and is obtained by noticing that,

$$\sum_{m=0}^5 3^m \binom{5}{m} = 2^{10}, \quad (7)$$

where $3^m \binom{5}{m}$ is the cardinality of weight- m error operators A'_k . More details on the explicit expressions for weight-0 and weight-1 appear in the Appendix A.

Encoding. The $[[5, 1, 3]]$ code is the smallest single-error correcting quantum code [20]. Of all QECCs that encode 1 qubit of data and correct all single-qubit errors, the $[[5, 1, 3]]$ is the most efficient, saturating the quantum Hamming bound. It encodes $k = 1$ qubit in $n = 5$ qubits. The cardinality of its stabilizer group \mathcal{S} is $|\mathcal{S}| = 2^{n-k} = 16$ and the set $\mathcal{B}_S^{[[5,1,3]]}$ of $n - k = 4$ group generators is given by [21],

$$\mathcal{B}_S^{[[5,1,3]]} \stackrel{\text{def}}{=} \{X^1 Z^2 Z^3 X^4, X^2 Z^3 Z^4 X^5, X^1 X^3 Z^4 Z^5, Z^1 X^2 X^4 Z^5\}. \quad (8)$$

The distance of the code is $d = 3$ and therefore the weight of the smallest error $A'_l A'_k$ that cannot be detected by the code is 3. Finally, we recall that it is a non-degenerate code since the smallest weight for elements of \mathcal{S} (other than identity) is 4 and therefore it is greater than the distance $d = 3$. The encoding for the $[[5, 1, 3]]$ code is given by [20],

$$|0\rangle \rightarrow |0_L\rangle = \frac{1}{4} \begin{bmatrix} |00000\rangle + |11000\rangle + |01100\rangle + |00110\rangle + |00011\rangle + |10001\rangle - |01010\rangle - |00101\rangle + \\ - |10010\rangle - |01001\rangle - |10100\rangle - |11110\rangle - |01111\rangle - |10111\rangle - |11011\rangle - |11101\rangle \end{bmatrix}, \quad (9)$$

and,

$$|1\rangle \rightarrow |1_L\rangle = \frac{1}{4} \begin{bmatrix} |11111\rangle + |00111\rangle + |10011\rangle + |11001\rangle + |11100\rangle + |01110\rangle - |10101\rangle - |11010\rangle + \\ - |01101\rangle - |10110\rangle - |01011\rangle - |00001\rangle - |10000\rangle - |01000\rangle - |00100\rangle - |00010\rangle \end{bmatrix}. \quad (10)$$

Recovery Operators. Recall that any error belonging to the Pauli group of n -qubits, $E \in \mathcal{P}_n$, can be written as,

$$E = i^\xi \sigma_{k_1}^1 \otimes \dots \otimes \sigma_{k_n}^n, \quad (11)$$

where $\xi = 0, 1, 2, 3$ and the superscripts on the $\sigma_{k_l}^l$ label the qubits $l = 1, \dots, n$. Furthermore, the subscripts take values $k_l = 0, x, y, z$ (therefore, $\sigma_0 \equiv I$, $\sigma_x \equiv X$, $\sigma_y \equiv Y$, $\sigma_z \equiv Z$) and $\sigma_0^l = I^l$ is the identity operator on the l^{th} qubit. Notice that since $\sigma_y^l = -i\sigma_x^l \sigma_z^l$, (11) can be rewritten as,

$$E = i^{\xi'} \sigma_x(a) \sigma_z(b), \quad (12)$$

where $a = a_1 \dots a_n$ and $b = b_1 \dots b_n$ are the bit strings of length n with,

$$\sigma_x(a) \equiv (\sigma_x^1)^{a_1} \otimes \dots \otimes (\sigma_x^n)^{a_n} \quad \text{and} \quad \sigma_z(b) \equiv (\sigma_z^1)^{b_1} \otimes \dots \otimes (\sigma_z^n)^{b_n}. \quad (13)$$

Although the factor $i^{\xi'}$ in (12) is needed to insure that \mathcal{P}_n is a group, in many discussions it is only necessary to work with the quotient group $\mathcal{P}_n / \{\pm I, \pm iI\}$.

There is a 1-1 correspondence between $\mathcal{P}_n / \{\pm I, \pm iI\}$ and the $2n$ -dimensional binary vector space F_2^{2n} whose elements are bit strings of length $2n$ [22]. A vector $v \in F_2^{2n}$ is denoted $v = (a|b)$, where $a = a_1 \dots a_n$ and $b = b_1 \dots b_n$ are bit strings of length n . Scalars take values in the Galois field $F_2 = \{0, 1\}$ and vector addition adds components modulo 2. In short, $E = i^{\xi'} \sigma_x(a) \sigma_z(b) \in \mathcal{P}_n \leftrightarrow v_l = (a_l|b_l) \in F_2^{2n}$. For a quantum stabilizer code \mathcal{C} with generators g_1, \dots, g_{n-k} and parity check matrix H , the error syndrome $S(E)$ for an error $E \in \mathcal{P}_n \leftrightarrow v_E = (a_E|b_E) \in F_2^{2n}$ is given by the bit string,

$$S(E) = H v_E = l_1 \dots l_{n-k}, \quad (14)$$

where,

$$l_j = H^T(j) \cdot v_E = \langle v_j, E \rangle, \quad (15)$$

with $v_j = (a_j|b_j)$ the image of the generators g_j and $\langle \cdot, \cdot \rangle$ the symbol for the symplectic inner product [22]. Furthermore, recall that errors with non-vanishing error syndrome are detectable and that a set of invertible error operators

$\mathcal{A}_{\text{correctable}}$ is correctable if the set given by $\mathcal{A}_{\text{correctable}}^\dagger \mathcal{A}_{\text{correctable}}$ is detectable [23]. It is straightforward, though tedious, to check that (see Appendix A),

$$S(A_l^\dagger A_k') \neq 0, \text{ with } l, k \in \{0, 1, \dots, 15\}, \quad (16)$$

where $S(A_k')$ is the error syndrome of the error operator A_k' defined as,

$$S(A_k') \stackrel{\text{def}}{=} H^{[[5,1,3]]} v_{A_k'}. \quad (17)$$

The quantity $H^{[[5,1,3]]}$ is the check matrix for the five-qubit code [21],

$$H^{[[5,1,3]]} \stackrel{\text{def}}{=} \left(\begin{array}{cccc|cccc} 1 & 1 & 0 & 0 & 0 & 0 & 1 & 0 & 1 \\ 0 & 1 & 1 & 0 & 0 & 1 & 0 & 0 & 1 & 0 \\ 0 & 0 & 1 & 1 & 0 & 0 & 1 & 0 & 0 & 1 \\ 0 & 0 & 0 & 1 & 1 & 1 & 0 & 1 & 0 & 0 \end{array} \right), \quad (18)$$

and $v_{A_k'}$ is the vector in the 10-dimensional binary vector space F_2^{10} corresponding to the error operator A_k' . The set of correctable error operators is given by,

$$\mathcal{A}_{\text{correctable}} = \{A_0', A_1', A_2', A_3', A_4', A_5', A_6', A_7', A_8', A_9', A_{10}', A_{11}', A_{12}', A_{13}', A_{14}', A_{15}'\} \subseteq \mathcal{A}, \quad (19)$$

where the cardinality of \mathcal{A} defining the channel in (6) equals 2^{10} . All weight zero and one error operators satisfy the error correction conditions [21, 24],

$$\langle i_L | A_l^\dagger A_m' | j_L \rangle = \alpha_{lm} \delta_{ij}, \quad (20)$$

for $l, m \in \{0, 1, \dots, 15\}$ and $i, j \in \{0, 1\}$ with $\langle i_L | j_L \rangle = \delta_{ij}$. The two sixteen-dimensional orthogonal subspaces \mathcal{V}^{0L} and \mathcal{V}^{1L} of \mathcal{H}_2^5 generated by the action of $\mathcal{A}_{\text{correctable}}$ on $|0_L\rangle$ and $|1_L\rangle$ are given by,

$$\mathcal{V}^{0L} = \text{Span} \left\{ |v_k^{0L}\rangle = \frac{A_k'}{\sqrt{p_k}} |0_L\rangle, \right\}, \quad (21)$$

with $k = 0, 1, \dots, 15$ and,

$$\mathcal{V}^{1L} = \text{Span} \left\{ |v_k^{1L}\rangle = \frac{A_k'}{\sqrt{p_k}} |1_L\rangle, \right\}, \quad (22)$$

respectively. Notice that $\langle v_l^{iL} | v_{l'}^{jL} \rangle = \delta_{ll'} \delta_{ij}$ with $l, l' \in \{0, 1, \dots, 15\}$ and $i, j \in \{0, 1\}$. Therefore, it follows that $\mathcal{V}^{0L} \oplus \mathcal{V}^{1L} = \mathcal{H}_2^5$. The recovery superoperator $\mathcal{R} \leftrightarrow \{R_l\}$ with $l = 1, \dots, 16$ is defined as [2],

$$R_l \stackrel{\text{def}}{=} V_l \sum_{i=0}^1 |v_l^{iL}\rangle \langle v_l^{iL}|, \quad (23)$$

where the unitary operator V_l is such that $V_l |v_l^{iL}\rangle = |i_L\rangle$ for $i \in \{0, 1\}$. Notice that (see Appendix A for the explicit expressions of recovery operators),

$$R_l \stackrel{\text{def}}{=} V_l \sum_{i=0}^1 |v_l^{iL}\rangle \langle v_l^{iL}| = |0_L\rangle \langle v_l^{0L}| + |1_L\rangle \langle v_l^{1L}|. \quad (24)$$

Notice that $\mathcal{R} \leftrightarrow \{R_l\}$ is a trace preserving quantum operation, $\sum_{l=1}^{16} R_l^\dagger R_l = I_{32 \times 32}$, since $\{|v_l^{iL}\rangle\}$ with $l = 1, \dots, 16$ and $i_L \in \{0, 1\}$ is an orthonormal basis for \mathcal{H}_2^5 . Finally, the action of this recovery operation \mathcal{R} on the map $\Lambda^{(5)}(\rho)$ in (6) yields,

$$\Lambda_{\text{recover}}^{(5)}(\rho) \equiv \left(\mathcal{R} \circ \Lambda^{(5)} \right) (\rho) \stackrel{\text{def}}{=} \sum_{k=0}^{2^{10}-1} \sum_{l=1}^{16} (R_l A_k') \rho (R_l A_k')^\dagger. \quad (25)$$

Entanglement Fidelity. Entanglement fidelity is a useful performance measure of the efficiency of quantum error correcting codes. It is a quantity that keeps track of how well the state and entanglement of a subsystem of a larger system are stored, without requiring the knowledge of the complete state or dynamics of the larger system. More precisely, the entanglement fidelity is defined for a mixed state $\rho = \sum_i p_i \rho_i = \text{tr}_{\mathcal{H}_R} |\psi\rangle\langle\psi|$ in terms of a purification $|\psi\rangle \in \mathcal{H} \otimes \mathcal{H}_R$ to a reference system \mathcal{H}_R . The purification $|\psi\rangle$ encodes all of the information in ρ . Entanglement fidelity is a measure of how well the channel Λ preserves the entanglement of the state \mathcal{H} with its reference system \mathcal{H}_R . The entanglement fidelity is defined as follows [19],

$$\mathcal{F}(\rho, \Lambda) \stackrel{\text{def}}{=} \langle\psi| (\Lambda \otimes I_{\mathcal{H}_R}) (|\psi\rangle\langle\psi|) |\psi\rangle, \quad (26)$$

where $|\psi\rangle$ is any purification of ρ , $I_{\mathcal{H}_R}$ is the identity map on $\mathcal{M}(\mathcal{H}_R)$ and $\Lambda \otimes I_{\mathcal{H}_R}$ is the evolution operator extended to the space $\mathcal{H} \otimes \mathcal{H}_R$, space on which ρ has been purified. If the quantum operation Λ is written in terms of its Kraus error operators $\{A_k\}$ as, $\Lambda(\rho) = \sum_k A_k \rho A_k^\dagger$, then it can be shown that [25],

$$\mathcal{F}(\rho, \Lambda) = \sum_k \text{tr}(A_k \rho) \text{tr}(A_k^\dagger \rho) = \sum_k |\text{tr}(\rho A_k)|^2. \quad (27)$$

This expression for the entanglement fidelity is very useful for explicit calculations. Finally, assuming that

$$\Lambda : \mathcal{M}(\mathcal{H}) \ni \rho \mapsto \Lambda(\rho) = \sum_k A_k \rho A_k^\dagger \in \mathcal{M}(\mathcal{H}), \quad \dim_{\mathbb{C}} \mathcal{H} = N \quad (28)$$

and choosing a purification described by a maximally entangled unit vector $|\psi\rangle \in \mathcal{H} \otimes \mathcal{H}$ for the mixed state $\rho = \frac{1}{\dim_{\mathbb{C}} \mathcal{H}} I_{\mathcal{H}}$, we obtain

$$\mathcal{F}\left(\frac{1}{N} I_{\mathcal{H}}, \Lambda\right) = \frac{1}{N^2} \sum_k |\text{tr} A_k|^2. \quad (29)$$

The expression in (29) represents the entanglement fidelity when no error correction is performed on the noisy channel Λ in (28).

Here we want to describe the action of $\mathcal{R} \circ \Lambda^{(5)}$ in (25) restricted to the code subspace \mathcal{C} . Note that the recovery operators can be expressed as,

$$R_{l+1} = R_l \frac{A'_l}{\sqrt{p_l}} = (|0_L\rangle\langle 0_L| + |1_L\rangle\langle 1_L|) \frac{A'_l}{\sqrt{p_l}}, \quad (30)$$

with $l \in \{0, \dots, 15\}$. Recalling that $A'_l = A_l'^\dagger$, it turns out that,

$$\langle i_L | R_{l+1} A'_k | j_L \rangle = \frac{1}{\sqrt{p_l}} \langle i_L | 0_L \rangle \langle 0_L | A_l'^\dagger A'_k | j_L \rangle + \frac{1}{\sqrt{p_l}} \langle i_L | 1_L \rangle \langle 1_L | A_l'^\dagger A'_k | j_L \rangle. \quad (31)$$

We now need to compute the 2×2 matrix representation $[R_l A'_k]_{|\mathcal{C}}$ of each $R_l A'_k$ with $l = 0, \dots, 15$ and $k = 0, \dots, 2^{10} - 1$ where,

$$[R_{l+1} A'_k]_{|\mathcal{C}} \stackrel{\text{def}}{=} \begin{pmatrix} \langle 0_L | R_{l+1} A'_k | 0_L \rangle & \langle 0_L | R_{l+1} A'_k | 1_L \rangle \\ \langle 1_L | R_{l+1} A'_k | 0_L \rangle & \langle 1_L | R_{l+1} A'_k | 1_L \rangle \end{pmatrix}. \quad (32)$$

For $l, k = 0, \dots, 15$, we note that $[R_{l+1} A'_k]_{|\mathcal{C}}$ becomes,

$$[R_{l+1} A'_k]_{|\mathcal{C}} = \begin{pmatrix} \langle 0_L | A_l'^\dagger A'_k | 0_L \rangle & 0 \\ 0 & \langle 1_L | A_l'^\dagger A'_k | 1_L \rangle \end{pmatrix} = \sqrt{\tilde{p}_l} \delta_{lk} \begin{pmatrix} 1 & 0 \\ 0 & 1 \end{pmatrix}, \quad (33)$$

while for any pair (l, k) with $l = 0, \dots, 15$ and $k > 15$, it follows that,

$$\langle 0_L | R_{l+1} A'_k | 0_L \rangle + \langle 1_L | R_{l+1} A'_k | 1_L \rangle = 0. \quad (34)$$

We conclude that the only matrices $[R_l A'_k]_{|\mathcal{C}}$ with non-vanishing trace are given by,

$$[R_s A'_{s-1}]_{|\mathcal{C}} = \sqrt{\tilde{p}_{s-1}} \begin{pmatrix} 1 & 0 \\ 0 & 1 \end{pmatrix}, \quad (35)$$

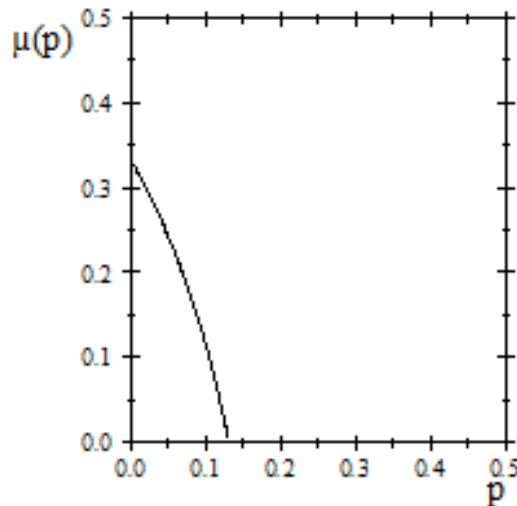


FIG. 1: Threshold curve for the five-qubit code.

with $s = 1, \dots, 16$. Therefore, the entanglement fidelity $\mathcal{F}^{[[5,1,3]]}(\mu, p)$ defined as,

$$\mathcal{F}^{[[5,1,3]]}(\mu, p) \stackrel{\text{def}}{=} \mathcal{F}^{[[5,1,3]]} \left(\frac{1}{2} I_{2 \times 2}, \mathcal{R} \circ \Lambda^{(5)} \right) = \frac{1}{(2)^2} \sum_{k=0}^{2^{10}-1} \sum_{l=1}^{16} \left| \text{tr} \left([R_l A'_k]_C \right) \right|^2, \quad (36)$$

results,

$$\mathcal{F}^{[[5,1,3]]}(\mu, p) = \sum_{m=0}^{15} \tilde{p}_m = p_{00}^4 p_0 + 3 [2p_{00}^3 p_{10} p_0 + 3p_{00}^2 p_{01} p_{10} p_0]. \quad (37)$$

Notice that the expression in (36) represents the entanglement fidelity after the error correction scheme provided by the five-qubit code is performed on the noisy channel $\Lambda^{(5)}$. The explicit expression for $\mathcal{F}^{[[5,1,3]]}(\mu, p)$ in (37) appears in Appendix A.

Note that for arbitrary memory parameter μ ,

$$\lim_{p \rightarrow 0} \mathcal{F}^{[[5,1,3]]}(\mu, p) = 1 \text{ and } \lim_{p \rightarrow 1} \mathcal{F}^{[[5,1,3]]}(\mu, p) = 0, \quad (38)$$

and for $\mu = 0$,

$$\mathcal{F}^{[[5,1,3]]}(0, p) = 4p^5 - 15p^4 + 20p^3 - 10p^2 + 1. \quad (39)$$

We recall that in general the application of a quantum error correcting code will lower the error probability as long as the probability of error on an unencoded qubit is less than a certain critical value (threshold probability). This threshold probability value depends on the code and above such critical value, the use of a coding scheme only makes the information corruption worse. Obviously, in order to make effective use of quantum error correction, a physical implementation of a channel with a sufficiently low error probability, as well as a code with a sufficiently high threshold is needed. For instance, the three-qubit repetition code improves the transmission accuracy when the probability of a bit flip on each qubit sent through the underlying channel is less than 0.5. For greater error probabilities, the error correction process is actually more likely to corrupt the data than unencoded transmission would be. In our analysis, the failure probability is represented by [26],

$$\mathcal{P}(\mu, p) \stackrel{\text{def}}{=} 1 - \mathcal{F}(\mu, p), \quad (40)$$

and it gives us an upper bound on the probability with which a generic encoded state will end up at a wrong state. Therefore, the five-qubit code is effective only if $\mathcal{P}^{[[5,1,3]]}(\mu, p) < p$. The effectiveness parametric region $\mathcal{D}^{[[5,1,3]]}$ for the five-qubit code is,

$$\mathcal{D}^{[[5,1,3]]} \stackrel{\text{def}}{=} \left\{ (\mu, p) \in [0, 1] \times [0, 1] : \mathcal{P}^{[[5,1,3]]}(\mu, p) < p \right\}. \quad (41)$$

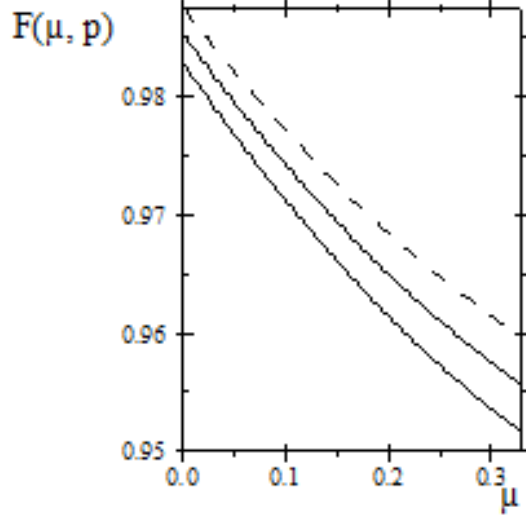


FIG. 2: $\mathcal{F}^{[[5,1,3]]}(\mu, p)$ vs. μ with $0 \leq \mu \leq 0.33$ (for $\mu > 0.33$, the error correction scheme is not effective anymore) for $p = 4.33 \times 10^{-2}$ (thick solid line), $p = 4 \times 10^{-2}$ (thin solid line) and $p = 3.67 \times 10^{-2}$ (dashed line).

For the five-qubit code applied for the correction of correlated depolarizing errors, it turns out that for increasing values of the memory parameter μ , the maximum values of the errors probabilities p for which the correction scheme is effective decrease. More generally, the threshold curve $\mu_{\text{threshold}}^{[[5,1,3]]} = \mu_{\text{threshold}}^{[[5,1,3]]}(p)$ defining the parametric region where QEC is effective is plotted in Figure 1. Furthermore, we point out that the presence of correlations in symmetric depolarizing errors does not improve the performance of the five-qubit code since $\mathcal{F}^{[[5,1,3]]}(\mu, p) \leq \mathcal{F}^{[[5,1,3]]}(0, p)$ for those (μ, p) -pairs belonging to the parametric region $\mathcal{D}^{[[5,1,3]]}$. Finally, the plots of $\mathcal{F}^{[[5,1,3]]}(\mu, p)$ vs. μ for $p = 4.33 \times 10^{-2}$, $p = 4 \times 10^{-2}$ and $p = 3.67 \times 10^{-2}$ are presented in Figure 2.

III. THE SEVEN-QUBIT CODE: SYMMETRIC ERROR PROBABILITIES AND CORRELATIONS

In this Section, we consider a depolarizing noisy quantum memory channel with symmetric error probabilities and QEC is performed via the $[[7, 1, 3]]$ -CSS stabilizer code. The performance of quantum error correcting codes is quantified by means of the entanglement fidelity $\mathcal{F}^{[[7,1,3]]}(\mu, p)$ as function of the error probability p and degree of memory μ .

Error Model. Consider seven qubits and correlated errors in a depolarizing quantum channel $\Lambda^{(7)}(\rho)$,

$$\Lambda^{(7)}(\rho) = \sum_{i_1, i_2, i_3, i_4, i_5, i_6, i_7=0}^3 p_{i_7|i_6} p_{i_6|i_5} p_{i_5|i_4} p_{i_4|i_3} p_{i_3|i_2} p_{i_2|i_1} p_{i_1} \left[A_{i_7} A_{i_6} A_{i_5} A_{i_4} A_{i_3} A_{i_2} A_{i_1} \rho A_{i_1}^\dagger A_{i_2}^\dagger A_{i_3}^\dagger A_{i_4}^\dagger A_{i_5}^\dagger A_{i_6}^\dagger A_{i_7}^\dagger \right], \quad (42)$$

where $A_0 \equiv I$, $A_1 \equiv X$, $A_2 \equiv Y$, $A_3 \equiv Z$ are the Pauli operators and the coefficients $p_{i_l|i_m}$ with $l, m \in \{0, 1, \dots, 7\}$ satisfying the normalization condition,

$$\sum_{i_1, i_2, i_3, i_4, i_5, i_6, i_7=0}^3 p_{i_7|i_6} p_{i_6|i_5} p_{i_5|i_4} p_{i_4|i_3} p_{i_3|i_2} p_{i_2|i_1} p_{i_1} = 1. \quad (43)$$

For the depolarizing channel $\Lambda^{(7)}(\rho)$, coefficients $p_{i_l|i_m}$ are explicitly defined in (5).

Error Operators. In an explicit way, the depolarizing channel $\Lambda^{(7)}(\rho)$ can be written as,

$$\Lambda^{(7)}(\rho) = \sum_{k=0}^{2^{14}-1} A'_k \rho A_k'^\dagger, \quad (44)$$

where A'_k are the enlarged error operators acting on the seven qubit quantum states. The cardinality of the error

operators defining $\Lambda^{(7)}(\rho)$ is 2^{14} and is obtained by noticing that,

$$\sum_{m=0}^7 3^m \binom{7}{m} = 2^{14}, \quad (45)$$

where $3^m \binom{7}{m}$ is the cardinality of weight- m error operators A'_k in (44).

Encoding. The Calderbank-Shor-Steane (CSS) codes are constructed from two classical binary codes \mathcal{C} and \mathcal{C}' that have the following properties [27, 28]: 1) \mathcal{C} and \mathcal{C}' are $[n, k, d]$ and $[n, k', d']$ codes, respectively; 2) $\mathcal{C}' \subset \mathcal{C}$; 3) \mathcal{C} and \mathcal{C}'_{\perp} (the dual code of \mathcal{C}') are both t -error correcting codes. For instance, in case of the seven-qubit code, the two classical codes are the $[7, 4, 3]$ binary Hamming code (\mathcal{C}) and the $[7, 3, 4]$ binary simplex code (\mathcal{C}'). The dual code \mathcal{C}'_{\perp} is the $[7, 4, 3]$ binary Hamming code. Thus \mathcal{C} and \mathcal{C}'_{\perp} are both 1-error correcting codes. In this case, $n = 7$, $k = 4$, $k' = 3$, $k - k' = 1$ so that 1 qubit is mapped into 7 qubits. The seven-qubit code is the simplest example of a CSS code. The five-qubit code introduced in the previous Section is the shortest possible quantum code to correct one error and is therefore of immense interest. Although the seven-qubit code is ostensibly more complicated than the five-qubit code, it is actually more useful in certain situations by virtue of being a CSS code. The CSS codes are a particularly interesting class of codes for two reasons. First, they are built using classical codes which have been more heavily studied than quantum codes, so it is fairly easy to construct useful quantum codes simply by looking at lists of classical codes. Second, because of the form of generators, the CSS codes are precisely those for which a CNOT applied between every pair of corresponding qubits in two blocks performs a valid fault-tolerant operation. This makes them particularly good candidates in fault-tolerant computation.

The $[[7, 1, 3]]$ -CSS code encodes $k = 1$ qubit in $n = 7$ qubits. The cardinality of its stabilizer group \mathcal{S} is $|\mathcal{S}| = 2^{n-k} = 64$ and the set $\mathcal{B}_S^{[[7,1,3]]}$ of $n - k = 6$ group generators is given by [21],

$$\mathcal{B}_S^{[[7,1,3]]} \stackrel{\text{def}}{=} \{X^4 X^5 X^6 X^7, X^2 X^3 X^6 X^7, X^1 X^3 X^5 X^7, Z^4 Z^5 Z^6 Z^7, Z^2 Z^3 Z^6 Z^7, Z^1 Z^3 Z^5 Z^7\}. \quad (46)$$

The distance of the code is $d = 3$ and therefore the weight of the smallest error $A_l^{\dagger} A'_k$ that cannot be detected by the code is 3. Finally, we recall that it is a non-degenerate code since the smallest weight for elements of \mathcal{S} (other than identity) is 4 and therefore it is greater than the distance $d = 3$. The encoding for the $[[7, 1, 3]]$ code is given by [21],

$$|0\rangle \rightarrow |0_L\rangle = \frac{1}{(\sqrt{2})^3} \left[\begin{array}{l} |0000000\rangle + |0110011\rangle + |1010101\rangle + |1100110\rangle + \\ + |0001111\rangle + |0111100\rangle + |1011010\rangle + |1101001\rangle \end{array} \right], \quad (47)$$

and,

$$|1\rangle \rightarrow |1_L\rangle = \frac{1}{(\sqrt{2})^3} \left[\begin{array}{l} |1111111\rangle + |1001100\rangle + |0101010\rangle + |0011001\rangle + \\ + |1110000\rangle + |1000011\rangle + |0100101\rangle + |0010110\rangle \end{array} \right]. \quad (48)$$

Recovery Operators. Recall that errors with non-vanishing error syndrome are detectable and that a set of invertible error operators $\mathcal{A}_{\text{correctable}}$ is correctable if the set given by $\mathcal{A}_{\text{correctable}}^{\dagger} \mathcal{A}_{\text{correctable}}$ is detectable [23]. It is straightforward, though tedious, to check that,

$$S(A_l^{\dagger} A'_k) \neq 0, \text{ with } l, k \in \{0, 1, \dots, 63\}, \quad (49)$$

where $S(A'_k)$ is the error syndrome of the error operator A'_k (see Appendix B for their explicit expressions) defined as [26],

$$S(A'_k) \stackrel{\text{def}}{=} H^{[[7,1,3]]} v_{A'_k}. \quad (50)$$

The quantity $H^{[[7,1,3]]}$ is the check matrix for the seven-qubit code [21],

$$H^{[[7,1,3]]} \stackrel{\text{def}}{=} \left(\begin{array}{cccccc|cccc} 1 & 1 & 1 & 1 & 0 & 0 & 0 & 0 & 0 & 0 & 0 & 0 & 0 & 0 & 0 & 0 \\ 1 & 1 & 0 & 0 & 1 & 1 & 0 & 0 & 0 & 0 & 0 & 0 & 0 & 0 & 0 & 0 \\ 1 & 0 & 1 & 0 & 1 & 0 & 1 & 0 & 0 & 0 & 0 & 0 & 0 & 0 & 0 & 0 \\ 0 & 0 & 0 & 0 & 0 & 0 & 0 & 0 & 1 & 1 & 1 & 1 & 0 & 0 & 0 & 0 \\ 0 & 0 & 0 & 0 & 0 & 0 & 0 & 0 & 1 & 1 & 0 & 0 & 1 & 1 & 0 & 0 \\ 0 & 0 & 0 & 0 & 0 & 0 & 0 & 0 & 1 & 0 & 1 & 0 & 1 & 0 & 1 & 0 \end{array} \right), \quad (51)$$

and $v_{A'_k}$ is the vector in the 14-dimensional binary vector space F_2^{14} corresponding to the error operator A'_k . The $[[7, 1, 3]]$ -code has distance 3 and therefore all errors $A' \equiv A'_l{}^\dagger A'_k$ with $l, k \in \{0, \dots, 2^{14} - 1\}$ of weight less than 3 satisfy the relation,

$$\langle i_L | A' | j_L \rangle = \alpha_{A'} \delta_{ij}, \quad (52)$$

and at least one error of weight 3 exists that violates it. It is straightforward, though tedious, to check that all 1- and 2-qubit error operators satisfy this equation (therefore, they are detectable). Instead, there are 3-qubit errors that do not satisfy (52). For instance, the error operator $X^1 X^2 X^3$ is such that $\langle 0_L | X^1 X^2 X^3 | 1_L \rangle = 1 \neq 0$. The $[[7, 1, 3]]$ -code corrects arbitrary 1-qubit errors, not arbitrary 2-qubit errors. In Appendix B, we introduce the Set-1 of correctable errors and explicitly show that they are detectable. It turns out that the set of correctable error operators is given by,

$$\mathcal{A}_{\text{correctable}} = \{A'_0, A'_1, \dots, A'_{21}, A'_{22}, \dots, A'_{63}\} \subseteq \mathcal{A}, \quad (53)$$

where the cardinality of \mathcal{A} equals 2^{14} . All weight-0, weight-1 and the 42 weight-2 above-mentioned error operators (see Appendix B) satisfy the error correction conditions,

$$\langle i_L | A'_l{}^\dagger A'_m | j_L \rangle = \alpha'_{lm} \delta_{ij}, \quad (54)$$

for $l, m \in \{0, 1, \dots, 63\}$ and $i, j \in \{0, 1\}$ with $\langle i_L | j_L \rangle = \delta_{ij}$.

In general, QEC protocols are symmetric with respect to the phase and bit bases and so enable the detection and correction of an equal number of phase and bit errors. In the CSS construction a pair of codes are used, one for correcting the bit flip errors and the other for correcting the phase flip errors. These codes can be chosen in such a way that the code correcting the phase flip errors has a larger distance than that of the code correcting the bit flip errors. Therefore, the resulting asymmetric quantum code has different error correcting capability for handling different type of errors. For instance, we emphasize that for the seven-qubit code there is some freedom in the selection of the set of correctable errors, even after the stabilizer generators have been specified [29]. The seven-qubit code may be designed to prioritize a certain error over the others (say Z errors over X and X errors over Y). For instance, an implementation which has no possibility at all of a Y error could use a code where the set of correctable errors was chosen to exclude corrections for Y . Optimizing the seven-qubit code to completely remove the ability to correct one error could lead to qualitatively different behavior, possibly even including better threshold values [29]. Instead, the five-qubit code (which is not a CSS code) corrects a unique symmetric set of errors. In what follows, first we will compute $\mathcal{F}_{\text{Set-1}}^{[[7, 1, 3]]}(\mu, p)$ assuming to correct the set of errors in (53); second, we will compute $\mathcal{F}_{\text{Set-2}}^{[[7, 1, 3]]}(\mu, p)$ assuming to correct the set of errors where we prioritize Z errors over X and X errors over Y .

A. Computation of $\mathcal{F}_{\text{Set-1}}^{[[7, 1, 3]]}(\mu, p)$

The two 64-dimensional orthogonal subspaces \mathcal{V}^{0_L} and \mathcal{V}^{1_L} of \mathcal{H}_2^7 generated by the action of $\mathcal{A}_{\text{correctable}}$ on $|0_L\rangle$ and $|1_L\rangle$ are given by,

$$\mathcal{V}^{0_L} = \text{Span} \left\{ |v_{l+1}^{0_L}\rangle = \frac{1}{\sqrt{p'_l}} A'_l |0_L\rangle \right\}, \quad (55)$$

with $l \in \{0, \dots, 63\}$ and,

$$\mathcal{V}^{1_L} = \text{Span} \left\{ |v_{l+1}^{1_L}\rangle = \frac{1}{\sqrt{p'_l}} A'_l |1_L\rangle \right\}, \quad (56)$$

respectively. Notice that $\langle v_l^{i_L} | v_{l'}^{j_L} \rangle = \delta_{ll'} \delta_{ij}$ with $l, l' \in \{0, \dots, 63\}$ and $i, j \in \{0, 1\}$. Therefore, it follows that $\mathcal{V}^{0_L} \oplus \mathcal{V}^{1_L} = \mathcal{H}_2^7$. The recovery superoperator $\mathcal{R} \leftrightarrow \{R_l\}$ with $l = 1, \dots, 64$ is defined as [2],

$$R_l \stackrel{\text{def}}{=} V_l \sum_{i=0}^1 |v_l^{i_L}\rangle \langle v_l^{i_L}|, \quad (57)$$

where the unitary operator V_l is such that $V_l |v_l^{iL}\rangle = |i_L\rangle$ for $i \in \{0, 1\}$. Notice that,

$$R_l \stackrel{\text{def}}{=} V_l \sum_{i=0}^1 |v_l^{iL}\rangle \langle v_l^{iL}| = |0_L\rangle \langle 0_L| + |1_L\rangle \langle 1_L|. \quad (58)$$

It turns out that the 64 recovery operators are given by,

$$R_{l+1} = R_l \frac{A'_l}{\sqrt{\tilde{p}'_l}} = (|0_L\rangle \langle 0_L| + |1_L\rangle \langle 1_L|) \frac{A'_l}{\sqrt{\tilde{p}'_l}}, \quad (59)$$

with $l \in \{0, \dots, 63\}$. Notice that $\mathcal{R} \leftrightarrow \{R_l\}$ is a trace preserving quantum operation, $\sum_{l=1}^{64} R_l^\dagger R_l = I_{128 \times 128}$ because $\{|v_l^{iL}\rangle\}$ with $l = 1, \dots, 64$ and $i_L \in \{0, 1\}$ is an orthonormal basis for \mathcal{H}_2^7 . Finally, the action of this recovery operation \mathcal{R} on the map $\Lambda^{(7)}(\rho)$ in (6) leads to,

$$\Lambda_{\text{recover}}^{(7)}(\rho) \equiv (\mathcal{R} \circ \Lambda^{(7)})(\rho) \stackrel{\text{def}}{=} \sum_{k=0}^{2^{14}-1} \sum_{l=1}^{64} (R_l A'_k) \rho (R_l A'_k)^\dagger. \quad (60)$$

Entanglement Fidelity. We want to describe the action of $\mathcal{R} \circ \Lambda^{(7)}$ restricted to the code subspace \mathcal{C} . Recalling that $A'_l = A_l^{\dagger}$, it turns out that,

$$\langle i_L | R_{l+1} A'_k | j_L \rangle = \frac{1}{\sqrt{\tilde{p}'_l}} \langle i_L | 0_L \rangle \langle 0_L | A_l^{\dagger} A'_k | j_L \rangle + \frac{1}{\sqrt{\tilde{p}'_l}} \langle i_L | 1_L \rangle \langle 1_L | A_l^{\dagger} A'_k | j_L \rangle. \quad (61)$$

We now need to compute the 2×2 matrix representation $[R_l A'_k]_{|\mathcal{C}}$ of each $R_l A'_k$ with $l = 0, \dots, 63$ and $k = 0, \dots, 2^{14} - 1$ where,

$$[R_{l+1} A'_k]_{|\mathcal{C}} \stackrel{\text{def}}{=} \begin{pmatrix} \langle 0_L | R_{l+1} A'_k | 0_L \rangle & \langle 0_L | R_{l+1} A'_k | 1_L \rangle \\ \langle 1_L | R_{l+1} A'_k | 0_L \rangle & \langle 1_L | R_{l+1} A'_k | 1_L \rangle \end{pmatrix}. \quad (62)$$

For $l, k = 0, \dots, 63$, we note that $[R_{l+1} A'_k]_{|\mathcal{C}}$ becomes,

$$[R_{l+1} A'_k]_{|\mathcal{C}} = \begin{pmatrix} \langle 0_L | A_l^{\dagger} A'_k | 0_L \rangle & 0 \\ 0 & \langle 1_L | A_l^{\dagger} A'_k | 1_L \rangle \end{pmatrix} = \sqrt{\tilde{p}'_l} \delta_{lk} \begin{pmatrix} 1 & 0 \\ 0 & 1 \end{pmatrix}, \quad (63)$$

while for any pair (l, k) with $l = 0, \dots, 63$ and $k > 63$, it follows that,

$$\langle 0_L | R_{l+1} A'_k | 0_L \rangle + \langle 1_L | R_{l+1} A'_k | 1_L \rangle = 0. \quad (64)$$

We conclude that the only matrices $[R_l A'_k]_{|\mathcal{C}}$ with non-vanishing trace are given by $[R_{l+1} A'_l]_{|\mathcal{C}}$ with $l = 0, \dots, 63$ where,

$$[R_{l+1} A'_l]_{|\mathcal{C}} = \sqrt{\tilde{p}'_l} \begin{pmatrix} 1 & 0 \\ 0 & 1 \end{pmatrix}. \quad (65)$$

Therefore, the entanglement fidelity $\mathcal{F}_{\text{Set-1}}^{[[7,1,3]]}(\mu, p)$ defined as,

$$\mathcal{F}_{\text{Set-1}}^{[[7, 1, 3]]}(\mu, p) \stackrel{\text{def}}{=} \mathcal{F}_{\text{Set-1}}^{[[7,1,3]]} \left(\frac{1}{2} I_{2 \times 2}, \mathcal{R} \circ \Lambda^{(7)} \right) = \frac{1}{(2)^2} \sum_{k=0}^{2^{14}-1} \sum_{l=1}^{64} \left| \text{tr} \left([R_l A'_k]_{|\mathcal{C}} \right) \right|^2, \quad (66)$$

becomes (the explicit expression for $\mathcal{F}_{\text{Set-1}}^{[[7,1,3]]}(\mu, p)$ is given in Appendix B),

$$\mathcal{F}_{\text{Set-1}}^{[[7,1,3]]}(\mu, p) = p_{00}^6 p_0 + 6p_{00}^5 p_{10} p_0 + 15p_{00}^4 p_{01} p_{10} p_0 + 6p_{00}^4 p_{10}^2 p_0 + 24p_{00}^3 p_{01} p_{10}^2 p_0 + 12p_{00}^2 p_{01}^2 p_{10}^2 p_0. \quad (67)$$

Note that for arbitrary degree of memory μ ,

$$\lim_{p \rightarrow 0} \mathcal{F}_{\text{Set-1}}^{[[7,1,3]]}(\mu, p) = 1 \text{ and, } \lim_{p \rightarrow 1} \mathcal{F}_{\text{Set-1}}^{[[7,1,3]]}(\mu, p) = 0, \quad (68)$$

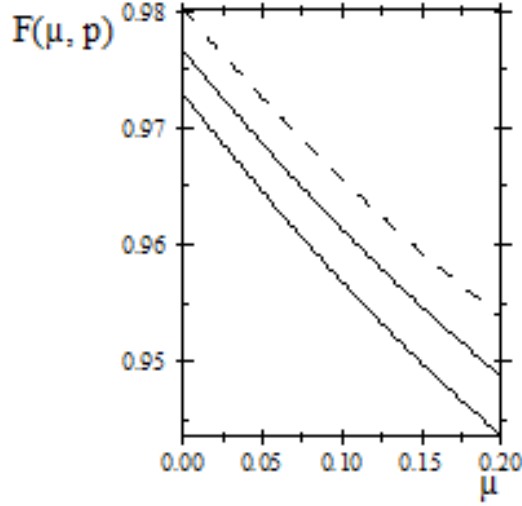


FIG. 3: $\mathcal{F}_{\text{Set-1}}^{[[7,1,3]]}(\mu, p)$ vs. μ for with $0 \leq \mu \leq 0.199$ (for $\mu > 0.199$, the error correction scheme is not effective anymore) $p = 4.33 \times 10^{-2}$ (thick solid line), $p = 4 \times 10^{-2}$ (thin solid line) and $p = 3.67 \times 10^{-2}$ (dashed line).

and for vanishing memory parameter $\mu = 0$,

$$\mathcal{F}_{\text{Set-1}}^{[[7,1,3]]}(0, p) = \frac{4}{3}p^7 - \frac{35}{3}p^6 + \frac{112}{3}p^5 - \frac{175}{3}p^4 + \frac{140}{3}p^3 - \frac{49}{3}p^2 + 1. \quad (69)$$

We emphasize that the presence of correlations in symmetric depolarizing errors does not improve the performance of the seven-qubit code since $\mathcal{F}_{\text{Set-1}}^{[[7,1,3]]}(\mu, p) \leq \mathcal{F}_{\text{Set-1}}^{[[7,1,3]]}(0, p)$ for those (μ, p) -pairs belonging to the parametric region $\mathcal{D}_{\text{Set-1}}^{[[7,1,3]]}$ where the correction scheme is effective,

$$\mathcal{D}_{\text{Set-1}}^{[[7,1,3]]} \stackrel{\text{def}}{=} \left\{ (\mu, p) \in [0, 1] \times [0, 1] : \mathcal{P}_{\text{Set-1}}^{[[7,1,3]]}(\mu, p) < p \right\}. \quad (70)$$

Furthermore, it turns out that $\mathcal{F}_{\text{Set-1}}^{[[7,1,3]]}(\mu, p) \leq \mathcal{F}^{[[5,1,3]]}(\mu, p)$ in $\mathcal{D}^{[[5,1,3]]} \cap \mathcal{D}_{\text{Set-1}}^{[[7,1,3]]}$ where the area of the parametric region $\mathcal{D}_{\text{Set-1}}^{[[7,1,3]]}$ is smaller than that of $\mathcal{D}^{[[7,1,3]]}$ (see Figure 4). The plots of $\mathcal{F}_{\text{Set-1}}^{[[7,1,3]]}(\mu, p)$ vs. μ for $p = 4.33 \times 10^{-2}$, $p = 4 \times 10^{-2}$ and $p = 3.67 \times 10^{-2}$ appear in Figure 3. For the seven-qubit code applied for the correction of correlated depolarizing errors in Set-1, it turns out that for increasing values of the memory parameter μ , the maximum values of the errors probabilities p for which the correction scheme is effective decrease. For instance, to $\mu_{\min} = 0$ corresponds a threshold $p_{\text{threshold}} \cong 7.63 \times 10^{-2}$ while to $\mu_{\max} \cong 0.199$ corresponds $p_{\text{threshold}} \cong 5.04 \times 10^{-4}$.

In the next Subsection, we will study the performance of the seven-qubit code assuming to correct a new set of correlated error operators. Moreover, we will compare the performance of the code in such two cases and discuss the change of the parametric regions where the quantum correction schemes are effective.

B. Computation of $\mathcal{F}_{\text{Set-2}}^{[[7, 1, 3]]}(\mu, p)$

Unlike the five-qubit code, the seven-qubit code corrects an asymmetric set of errors. In what follows, we choose the set of correctable errors to prioritize Z errors over X errors over Y errors. Said otherwise, we construct the set of correctable errors by proceeding in increasing order from single-qubit errors to errors of higher weight. Within each level (weight) of errors, we include those that incorporate the most Z errors first. In other words, the sets of weight-0 and weight-1 correctable errors are given in (B1) and (B2), respectively (see Appendix B). Following the line of reasoning presented in the previous Subsection, after some algebra it turns out that

$$\begin{aligned} \mathcal{F}_{\text{Set-2}}^{[[7,1,3]]}(\mu, p) = & p_{00}^6 p_0 + 6p_{00}^5 p_{10} p_0 + 15p_{00}^4 p_{01} p_{10} p_0 + 2p_{00}^4 p_{10} p_0 (p_{11} + 2p_{10}) + \\ & + 4p_{00}^3 p_{01} p_{10} p_0 (5p_{10} + p_{11}) + 12p_{00}^2 p_{01}^2 p_{10}^2 p_0. \end{aligned} \quad (71)$$

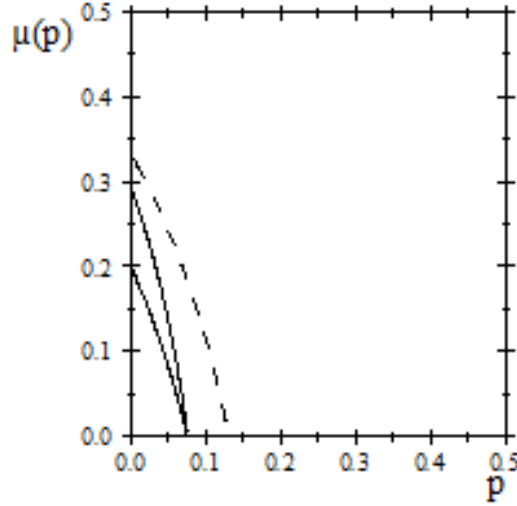


FIG. 4: Symmetric Case: Threshold curves $\mu_{\text{threshold}}^{[[5,1,3]]}(p)$ (dashed line), $\mu_{\text{threshold, Set-2}}^{[[7,1,3]]}(p)$ (thin solid line) and $\mu_{\text{threshold, Set-1}}^{[[7,1,3]]}(p)$ (thick solid line) vs. p .

From (71) and (67) (see also Appendix B), we obtain

$$\mathcal{F}_{\text{Set-2}}^{[[7,1,3]]}(\mu, p) - \mathcal{F}_{\text{Set-1}}^{[[7,1,3]]}(\mu, p) = (p_{11} - p_{10}) (2p_{00}^4 p_{10} p_0 + 4p_{00}^3 p_{01} p_{10} p_0) \geq 0, \quad (72)$$

with $(p_{11} - p_{10}) = \mu \geq 0$. The explicit expression for $\mathcal{F}_{\text{Set-2}}^{[[7,1,3]]}(\mu, p)$ appears in Appendix B. In absence of correlations and considering symmetric error probabilities, the two entanglement fidelities are the same. Therefore, we conclude that in the presence of memory effects, it does matter which set of errors we choose to correct, even limiting our analysis to symmetric error probabilities. We will see that the freedom of such choice becomes even more important when combining memory effects and asymmetric error probabilities.

For the seven-qubit code applied for the correction of correlated depolarizing errors in Set-2, it turns out that for increasing values of the memory parameter μ , the maximum values of the errors probabilities p for which the correction scheme is effective decrease. For instance, to $\mu_{\text{min}} = 0$ corresponds a threshold $p_{\text{threshold}} \cong 7.63 \times 10^{-2}$ while to $\mu_{\text{max}} \cong 0.29$ corresponds $p_{\text{threshold}} \cong 1.95 \times 10^{-3}$.

In conclusion, it follows that in the presence of correlated and symmetric depolarizing errors, the performances of both the five and the seven-qubit quantum codes are lowered. Furthermore, the five-qubit code is characterized by a parametric region (where its correction scheme is effective) that is larger than the one provided by the seven-qubit code (for both selected sets of correctable errors). Furthermore, in the parametric region where both error correction schemes are effective, the five-qubit code outperforms the seven-qubit code.

In the next Section, we will discover that the situation is slightly different when considering asymmetries and memory effects in depolarizing channels.

IV. THE FIVE AND SEVEN-QUBIT CODES: ASYMMETRIC ERROR PROBABILITIES AND CORRELATIONS

In this Section, we study the performance of the $[[5, 1, 3]]$ and $[[7, 1, 3]]$ quantum error correcting codes with respect to asymmetric error probabilities ($p = p_X + p_Y + p_Z$ with $p_X \neq p_Y \neq p_Z$) and correlated noise errors in a quantum depolarizing channel.

A. The Five-Qubit Code

In our following discussion, we will assume that the error probability p may be written as,

$$p = p_X + p_Y + p_Z, \quad (73)$$

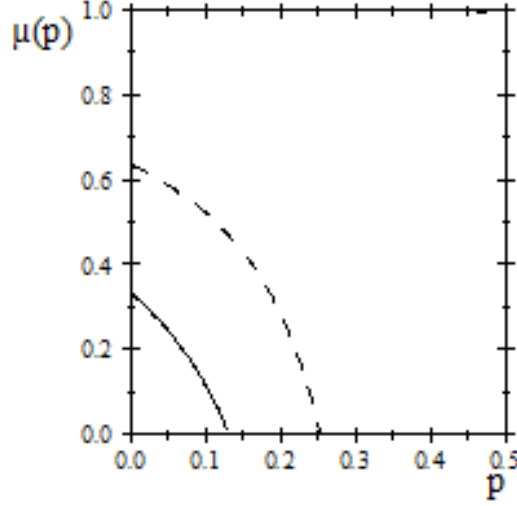


FIG. 5: Asymmetric Case: Threshold curves $\mu_{\text{threshold, Set-2}}^{[[7,1,3]]}(p)$ (dashed line) and $\mu_{\text{threshold}}^{[[5,1,3]]}(p)$ (thin solid line) vs. p .

where,

$$p_X = \alpha_X p, p_Y = \alpha_Y p, p_Z = \alpha_Z p, \quad (74)$$

with $\alpha_X + \alpha_Y + \alpha_Z = 1$. Notice that in the symmetric case, we simply have $\alpha_X = \alpha_Y = \alpha_Z = \frac{1}{3}$. Following the line of reasoning presented in Section II, it turns out that the $\mathcal{F}_{\text{asymmetric}}^{[[5,1,3]]}(\mu, p)$ becomes,

$$\begin{aligned} \mathcal{F}_{\text{asymmetric}}^{[[5,1,3]]}(\mu, p) = & p_{00}^4 p_0 + [p_{00}^3 p_{10} p_0 + 3p_{00}^2 p_{01} p_{10} p_0 + p_{00}^3 p_{01} p_1] + \\ & [p_{00}^3 p_{20} p_0 + 3p_{00}^2 p_{02} p_{20} p_0 + p_{00}^3 p_{02} p_2] + [p_{00}^3 p_{30} p_0 + 3p_{00}^2 p_{03} p_{30} p_0 + p_{00}^3 p_{03} p_3], \end{aligned} \quad (75)$$

where,

$$\begin{aligned} p_0 &= 1 - p, p_1 = \alpha_X p, p_2 = \alpha_Y p, p_3 = \alpha_Z p, p_{00} = (1 - \mu)(1 - p) + \mu, \\ p_{01} &= p_{02} = p_{03} = (1 - \mu)(1 - p), p_{10} = \alpha_X p(1 - \mu), \\ p_{20} &= \alpha_Y p(1 - \mu), p_{30} = \alpha_Z p(1 - \mu). \end{aligned} \quad (76)$$

After some straightforward algebra, $\mathcal{F}_{\text{asymmetric}}^{[[5, 1, 3]]}(\mu, p)$ in (75) may be written as,

$$\mathcal{F}_{\text{asymmetric}}^{[[5,1,3]]}(\mu, p) = p_{00}^4 p_0 + p_{00}^3 p_0 (p_{10} + p_{20} + p_{30}) + 3p_{00}^2 p_{01} p_0 (p_{10} + p_{20} + p_{30}) + p_{00}^3 p_{01} (p_1 + p_2 + p_3). \quad (77)$$

Recalling that in the symmetric case $p_1 = p_2 = p_3 = \frac{p}{3}$, $p_{10} = p_{20} = p_{30} = \frac{p}{3}(1 - \mu)$ and substituting (76) in (77), it follows that

$$\mathcal{F}_{\text{asymmetric}}^{[[5,1,3]]}(\mu, p) = \mathcal{F}_{\text{symmetric}}^{[[5,1,3]]}(\mu, p). \quad (78)$$

Therefore, we conclude that the performance of the five-qubit code cannot be enhanced in the case of asymmetric error probabilities in the depolarizing channel. This result was somehow expected since the five-qubit code corrects a unique and symmetric set of error operators.

B. The Seven-Qubit Code

Following the line of reasoning presented in Section III, it turns out that the entanglement fidelity $\mathcal{F}_{\text{asymmetric}}^{[[7,1,3]]}(\mu, p)$ evaluated assuming to correct the Set-2 of error operators becomes,

$$\begin{aligned} \mathcal{F}_{\text{asymmetric}}^{[[7,1,3]]}(\mu, p) = & p_{00}^6 p_0 + 2p_{00}^5 p_{01} (p_1 + p_2 + p_3) + 5p_{00}^4 p_{01} p_0 (p_{10} + p_{20} + p_{30}) + p_{00}^4 p_0 (2p_{30} p_{33} + p_{30}^2 + 3p_{10} p_{31}) + \\ & + p_{00}^3 p_{01} p_{30} p_0 (8p_{30} + 4p_{33} + 12p_{10}) + 6p_{00}^2 p_{01}^2 p_{30} p_0 (p_{30} + p_{10}), \end{aligned} \quad (79)$$

where,

$$\begin{aligned} p_0 &= 1 - p, p_1 = \alpha_X p, p_2 = \alpha_Y p, p_3 = \alpha_Z p, p_{00} = (1 - \mu)(1 - p) + \mu, \\ p_{01} &= p_{02} = p_{03} = (1 - \mu)(1 - p), p_{10} = \alpha_X p(1 - \mu), p_{20} = \alpha_Y p(1 - \mu), p_{30} = \alpha_Z p(1 - \mu), \\ p_{31} &= p_{30} = \alpha_Z p(1 - \mu), p_{33} = \alpha_Z p(1 - \mu) + \mu. \end{aligned} \quad (80)$$

Notice that for $p_X = p_Y = p_Z = \frac{p}{3}$, $\mathcal{F}_{\text{asymmetric}}^{[[7,1,3]]}(\mu, p)$ equals $\mathcal{F}_{\text{symmetric}}^{[[7,1,3]]}(\mu, p)$. In absence of correlations, the entanglement fidelity $\mathcal{F}_{\text{asymmetric}}^{[[7,1,3]]}$ becomes,

$$\mathcal{F}_{\text{asymmetric}}^{[[7,1,3]]}(0, p) = (1 - p)^7 + 7p(1 - p)^6 + 21p^2(1 - p)^5 [\alpha_Z^2 + \alpha_X \alpha_Z]. \quad (81)$$

The general expression of $\mathcal{F}_{\text{asymmetric}}^{[[7,1,3]]}(\mu, p)$ is given in Appendix C. We point out that in the absence of correlations but with asymmetric error probabilities, the seven-qubit code can outperforms the five-qubit code,

$$\mathcal{F}_{\text{asymmetric}}^{[[7,1,3]]}(0, p) \geq \mathcal{F}_{\text{asymmetric}}^{[[5,1,3]]}(0, p) \equiv \mathcal{F}_{\text{symmetric}}^{[[5,1,3]]}(0, p). \quad (82)$$

In Figure 5, we plot the threshold curves $\mu_{\text{threshold}}^{[[7,1,3]]}(p)$ and $\mu_{\text{threshold}}^{[[5,1,3]]}(p)$ versus p in the case case of asymmetric error probabilities. Asymmetries in the error probabilities enlarge the parametric regions where the seven-qubit code is effective for error correction. Furthermore, comparing the performances of such codes on a common region where they are both effective, the seven-qubit code turns out to outperform the five-qubit code in the presence of asymmetries and correlations. In Figure 6, we plot $\mathcal{F}_{\text{asymmetric}}^{[[7,1,3]]}(\mu, p)$, $\mathcal{F}_{\text{symmetric}}^{[[5,1,3]]}(\mu, p) = \mathcal{F}_{\text{asymmetric}}^{[[5,1,3]]}(\mu, p)$ and $\mathcal{F}_{\text{symmetric}}^{[[7,1,3]]}(\mu, p)$ versus the memory parameter μ for $p = 4 \times 10^{-2}$ and $\alpha_Z = 25\alpha$, $\alpha_X = 5\alpha$ and $\alpha_Y = \alpha$ with $\alpha_X + \alpha_Y + \alpha_Z = 1$.

V. FINAL REMARKS

In this article, we have studied the performance of common quantum stabilizer codes in the presence of asymmetric and correlated errors. Specifically, we considered the depolarizing noisy quantum memory channel and performed quantum error correction via the five and seven-qubit stabilizer codes. We have shown that memory effects in the error models combined with asymmetries in the error probabilities can produce relevant changes in the performances of quantum error correction schemes by qualitatively affecting the threshold error probability values for which the codes are effective. In summary, we have uncovered the following findings:

1. In the presence of correlated and symmetric depolarizing errors, the performances of both the five and the seven-qubit quantum stabilizer codes are lowered for fixed values of the degree of memory μ . Furthermore, such error correction schemes only work for low values of μ .
2. In the presence of correlated and symmetric depolarizing errors, the five-qubit code is characterized by a parametric region (where its correction scheme is effective) that is larger than the one provided by the seven-qubit code. Furthermore, in the parametric region where both error correction schemes are effective, the five-qubit code outperforms the seven-qubit code.
3. The asymmetry in the error probabilities does not affect the performance of the five-qubit code quantified in terms of its entanglement fidelity. On the contrary, it does affect the performance of the seven-qubit code which is less effective when considering correlated and symmetric depolarizing errors. This peculiar effect is rooted in the stabilizer structure of the CSS seven-qubit code: it is a consequence of the freedom in selecting the set of correctable error operators even after the stabilizer generators have been specified.

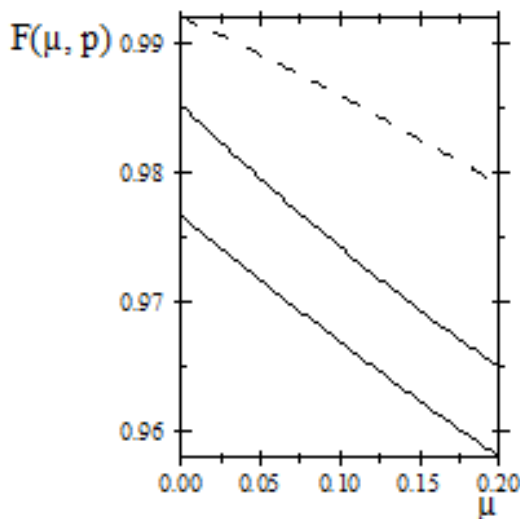


FIG. 6: $\mathcal{F}_{\text{asymmetric}}^{[[7,1,3]]}(\mu, p)$ (dashed line), $\mathcal{F}_{\text{asymmetric}}^{[[5,1,3]]} = \mathcal{F}_{\text{symmetric}}^{[[5,1,3]]}(\mu, p)$ (thin solid line) and $\mathcal{F}_{\text{symmetric}}^{[[7,1,3]]}(\mu, p)$ (thick solid line) vs. μ with $0 \leq \mu \lesssim 0.199$ (where both error correction schemes are effective) for $p = 4 \times 10^{-2}$ with $\alpha_Z = 25\alpha$, $\alpha_X = 5\alpha$ and $\alpha_Y = \alpha$.

4. The performance of the seven-qubit code significantly improves when considering correlated and asymmetric depolarizing errors. Furthermore, in such case it is also characterized by higher (than the one provided by the five-qubit code) error probability threshold values. This result confirms that in order to make effective use of quantum error correction, a physical implementation of a channel with a sufficiently low error probability, as well as a code with sufficiently high threshold probability is needed [30].

We conclude that in order to optimize the seven-qubit code performance, it is very important to know the experimental details of the physical implementation of the quantum memory channel being considered. Furthermore, in order to make effective use of quantum error correction, a more detailed analysis of the physical noise models for various qubit implementations is needed. This requirement, as we have shown, becomes even more pressing when dealing with noise models where memory effects are combined with asymmetries in the error probabilities.

Acknowledgments

C. C. thanks C. Lupo and L. Memarzadeh for useful comments. C. C. is also grateful to V. Aggarwal and R. Calderbank for their kind hospitality and useful discussions during his visit at The Program in Applied and Computational Mathematics at Princeton University. This work was supported by the European Community's Seventh Framework Program under grant agreement 213681 (CORNER Project; FP7/2007-2013).

Appendix A: The Five-Qubit Code

In this Appendix, we briefly discuss few technical details omitted in the manuscript concerning the application of the five-qubit code to the depolarizing memory channel with both symmetric and asymmetric error probabilities.

Error Operators. The weight zero and one quantum error operators in $\Lambda^{(5)}(\rho)$ in (6) are given by,

$$\begin{aligned}
A'_0 &= \sqrt{\tilde{p}_0} I^1 \otimes I^2 \otimes I^3 \otimes I^4 \otimes I^5, A'_1 = \sqrt{\tilde{p}_1} X^1 \otimes I^2 \otimes I^3 \otimes I^4 \otimes I^5, A'_2 = \sqrt{\tilde{p}_2} I^1 \otimes X^2 \otimes I^3 \otimes I^4 \otimes I^5, \\
A'_3 &= \sqrt{\tilde{p}_3} I^1 \otimes I^2 \otimes X^3 \otimes I^4 \otimes I^5, A'_4 = \sqrt{\tilde{p}_4} I^1 \otimes I^2 \otimes I^3 \otimes X^4 \otimes I^5, A'_5 = \sqrt{\tilde{p}_5} I^1 \otimes I^2 \otimes I^3 \otimes I^4 \otimes X^5, \\
A'_6 &= \sqrt{\tilde{p}_6} Y^1 \otimes I^2 \otimes I^3 \otimes I^4 \otimes I^5, A'_7 = \sqrt{\tilde{p}_7} I^1 \otimes Y^2 \otimes I^3 \otimes I^4 \otimes I^5, A'_8 = \sqrt{\tilde{p}_8} I^1 \otimes I^2 \otimes Y^3 \otimes I^4 \otimes I^5, \\
A'_9 &= \sqrt{\tilde{p}_9} I^1 \otimes I^2 \otimes I^3 \otimes Y^4 \otimes I^5, A'_{10} = \sqrt{\tilde{p}_{10}} I^1 \otimes I^2 \otimes I^3 \otimes I^4 \otimes Y^5, A'_{11} = \sqrt{\tilde{p}_{11}} Z^1 \otimes I^2 \otimes I^3 \otimes I^4 \otimes I^5, \\
A'_{12} &= \sqrt{\tilde{p}_{12}} I^1 \otimes Z^2 \otimes I^3 \otimes I^4 \otimes I^5, A'_{13} = \sqrt{\tilde{p}_{13}} I^1 \otimes I^2 \otimes Z^3 \otimes I^4 \otimes I^5, A'_{14} = \sqrt{\tilde{p}_{14}} I^1 \otimes I^2 \otimes I^3 \otimes Z^4 \otimes I^5, \\
A'_{15} &= \sqrt{\tilde{p}_{15}} I^1 \otimes I^2 \otimes I^3 \otimes I^4 \otimes Z^5,
\end{aligned} \tag{A1}$$

where the coefficients \tilde{p}_l with $l = 0, \dots, 15$ results,

$$\begin{aligned}
\tilde{p}_0 &= p_{00}^4 p_0, \tilde{p}_1 = p_{00}^3 p_{10} p_0, \tilde{p}_2 = p_{00}^2 p_{01} p_{10} p_0, \tilde{p}_3 = p_{00}^2 p_{01} p_{10} p_0, \tilde{p}_4 = p_{00}^2 p_{01} p_{10} p_0, \tilde{p}_5 = p_{00}^3 p_{01} p_1, \\
\tilde{p}_6 &= p_{00}^3 p_{20} p_0, \tilde{p}_7 = p_{00}^2 p_{02} p_{20} p_0, \tilde{p}_8 = p_{00}^2 p_{02} p_{20} p_0, \tilde{p}_9 = p_{00}^2 p_{02} p_{20} p_0, \tilde{p}_{10} = p_{00}^3 p_{02} p_2, \\
\tilde{p}_{11} &= p_{00}^3 p_{30} p_0, \tilde{p}_{12} = p_{00}^2 p_{03} p_{30} p_0, \tilde{p}_{13} = p_{00}^2 p_{03} p_{30} p_0, \tilde{p}_{14} = p_{00}^2 p_{03} p_{30} p_0, \tilde{p}_{15} = p_{00}^3 p_{03} p_3,
\end{aligned} \tag{A2}$$

with,

$$\begin{aligned}
p_0 &= 1 - p, p_1 = p_2 = p_3 = \frac{p}{3}, p_{00} = (1 - \mu)(1 - p) + \mu, \\
p_{01} &= p_{02} = p_{03} = (1 - \mu)(1 - p), p_{10} = p_{20} = p_{30} = \frac{p}{3}(1 - \mu).
\end{aligned} \tag{A3}$$

Detectable Errors. Recall that an error operator A'_k is detectable by the code \mathcal{C} if and only if

$$P_{\mathcal{C}} A'_k P_{\mathcal{C}} = \lambda_{A'_k} P_{\mathcal{C}}, \tag{A4}$$

for some $\lambda_{A'_k}$ where $P_{\mathcal{C}} \stackrel{\text{def}}{=} |0_L\rangle\langle 0_L| + |1_L\rangle\langle 1_L|$ is the projector on the code space. On the contrary, a set of error operators $\mathcal{A} = \{A'_l\}$ is correctable if and only if

$$P_{\mathcal{C}} A_m^\dagger A'_n P_{\mathcal{C}} = \lambda_{mn} P_{\mathcal{C}}, \tag{A5}$$

for any pair of error operators in \mathcal{A} where λ_{mn} define a positive semi-definite Hermitian matrix. We emphasize that the notion of *correctability* depends on all the errors in the set under consideration and, unlike *detectability*, cannot be applied to individual errors. For invertible error operators (such as the ones considered here), there is a simple relationship between detectability and correctability. A set \mathcal{A} is correctable if and only if the operators in the set $\mathcal{A}^\dagger \mathcal{A} \stackrel{\text{def}}{=} \{A_1^\dagger A_2 : A_i \in \mathcal{A}\}$ are detectable. It would be awfully tedious to identify either detectable errors or sets of correctable errors by means of (A4) and (A5) for the five and seven-qubit codes characterized by the codewords in (9) and (47), respectively. However, the quantum stabilizer formalism allows to simplify such task. This is a consequence of the fact that by means of such formalism it is sufficient to study the effect of the error operators on the generators of the stabilizer and not on the codewords themselves. In our work, we have made use of the stabilizer formalism together with the simple relationship between detectability and correctability for invertible error operators in order to identify sets of correctable and detectable errors.

It is known that errors with non-vanishing error syndrome are detectable. It is straightforward to check that,

$$S(A_l^\dagger A'_k) \neq 0, \text{ with } l, k \in \{0, 1, \dots, 15\}, \tag{A6}$$

where $S(A'_k)$ is the error syndrome of the error operator A'_k defined as,

$$S(A'_k) \stackrel{\text{def}}{=} H^{[[5,1,3]]} v_{A'_k}. \tag{A7}$$

The quantity $H^{[[5,1,3]]}$ is the check matrix for the five-qubit code in (18) and $v_{A'_k}$ is the vector in the 10-dimensional binary vector space F_2^{10} corresponding to the error operator A'_k . For instance, considering $k \in \{0, 1, \dots, 15\}$, we obtain

$$\begin{aligned} v_I &= (00000|00000), v_{X^1} = (10000|00000), v_{X^2} = (01000|00000), v_{X^3} = (00100|00000), \\ v_{X^4} &= (00010|00000), v_{X^5} = (00001|00000), v_{Z^1} = (00000|10000), v_{Z^2} = (00000|01000), \\ v_{Z^3} &= (00000|00100), v_{Z^4} = (00000|00010), v_{Z^5} = (00000|00001), v_{Y^1} = (10000|10000), \\ v_{Y^2} &= (01000|01000), v_{Y^3} = (00100|00100), v_{Y^4} = (00010|00010), v_{Y^5} = (00001|00001), \end{aligned} \quad (\text{A8})$$

and the error syndromes become,

$$\begin{aligned} S(I) &= 0000, S(X^1) = 1000, S(X^2) = 1100, S(X^3) = 0110, S(X^4) = 0011, S(X^5) = 0001, \\ S(Z^1) &= 0101, S(Z^2) = 0010, S(Z^3) = 1001, S(Z^4) = 0100, S(Z^5) = 1010, \\ S(Y^1) &= 1101, S(Y^2) = 1110, S(Y^3) = 1111, S(Y^4) = 0111, S(Y^5) = 1011. \end{aligned} \quad (\text{A9})$$

For a non-degenerate quantum stabilizer code, linearly independent correctable errors have unequal error syndromes. This necessary (but not sufficient) requirement for a set of correctable errors appears fulfilled in (A9). Finally, following the above-mentioned line of reasoning, we can show that (A6) is fulfilled.

Recovery Operators. From (24), it follows that the sixteen recovery operators are given by,

$$\begin{aligned} R_1 &= |0_L\rangle\langle 0_L| + |1_L\rangle\langle 1_L|, R_2 = R_1 X^1, R_3 = R_1 X^2, R_4 = R_1 X^3, R_5 = R_1 X^4, R_6 = R_1 X^5, \\ R_7 &= R_1 Y^1, R_8 = R_1 Y^2, R_9 = R_1 Y^3, R_{10} = R_1 Y^4, R_{11} = R_1 Y^5, \\ R_{12} &= R_1 Z^1, R_{13} = R_1 Z^2, R_{14} = R_1 Z^3, R_{15} = R_1 Z^4, R_{16} = R_1 Z^5. \end{aligned} \quad (\text{A10})$$

Entanglement Fidelity. The explicit expression for the entanglement fidelity $\mathcal{F}^{[[5,1,3]]}(\mu, p)$ in (37) is given by,

$$\begin{aligned} \mathcal{F}^{[[5,1,3]]}(\mu, p) &= \mu^4 (4p^5 - 7p^4 + 3p^3) + \mu^3 (-16p^5 + 36p^4 - 26p^3 + 6p^2) + \\ &+ \mu^2 (24p^5 - 66p^4 + 63p^3 - 24p^2 + 3p) + \mu (-16p^5 + 52p^4 - 60p^3 + 28p^2 - 4p) + \\ &+ (4p^5 - 15p^4 + 20p^3 - 10p^2 + 1). \end{aligned} \quad (\text{A11})$$

Appendix B: On the Seven-Qubit Code

In this Appendix, we briefly discuss few technical details omitted in the manuscript concerning the application of the seven-qubit code to the depolarizing memory channel with both symmetric and asymmetric error probabilities.

Error Operators (Set-1). The set of correctable error operators (Set-1) is explicitly defined by 64 error operators. The only weight-0 error operator is given by,

$$A'_0 = \sqrt{\tilde{p}'_0} I^1 \otimes I^2 \otimes I^3 \otimes I^4 \otimes I^5 \otimes I^6 \otimes I^7 \equiv \sqrt{\tilde{p}'_0} I. \quad (\text{B1})$$

The 21 weight-1 error (correctable) operators are given by,

$$\begin{aligned} A'_1 &= \sqrt{\tilde{p}'_1} X^1, A'_2 = \sqrt{\tilde{p}'_2} X^2, A'_3 = \sqrt{\tilde{p}'_3} X^3, A'_4 = \sqrt{\tilde{p}'_4} X^4, A'_5 = \sqrt{\tilde{p}'_5} X^5, \\ A'_6 &= \sqrt{\tilde{p}'_6} X^6, A'_7 = \sqrt{\tilde{p}'_7} X^7, A'_8 = \sqrt{\tilde{p}'_8} Y^1, A'_9 = \sqrt{\tilde{p}'_9} Y^2, A'_{10} = \sqrt{\tilde{p}'_{10}} Y^3, \\ A'_{11} &= \sqrt{\tilde{p}'_{11}} Y^4, A'_{12} = \sqrt{\tilde{p}'_{12}} Y^5, A'_{13} = \sqrt{\tilde{p}'_{13}} Y^6, A'_{14} = \sqrt{\tilde{p}'_{14}} Y^7, A'_{15} = \sqrt{\tilde{p}'_{15}} Z^1, \\ A'_{16} &= \sqrt{\tilde{p}'_{16}} Z^2, A'_{17} = \sqrt{\tilde{p}'_{17}} Z^3, A'_{18} = \sqrt{\tilde{p}'_{18}} Z^4, A'_{19} = \sqrt{\tilde{p}'_{19}} Z^5, A'_{20} = \sqrt{\tilde{p}'_{20}} Z^6, A'_{21} = \sqrt{\tilde{p}'_{21}} Z^7. \end{aligned} \quad (\text{B2})$$

Finally, the 42 weight-2 (correctable) error operators are,

$$\begin{aligned}
A'_{22} &= \sqrt{\tilde{p}'_{22}}X^1Z^2, A'_{23} = \sqrt{\tilde{p}'_{23}}X^1Z^3, A'_{24} = \sqrt{\tilde{p}'_{24}}X^1Z^4, A'_{25} = \sqrt{\tilde{p}'_{25}}X^1Z^5, A'_{26} = \sqrt{\tilde{p}'_{26}}X^1Z^6, \\
A'_{27} &= \sqrt{\tilde{p}'_{27}}X^1Z^7, A'_{28} = \sqrt{\tilde{p}'_{28}}Z^1X^2, A'_{29} = \sqrt{\tilde{p}'_{29}}X^2Z^3, A'_{30} = \sqrt{\tilde{p}'_{30}}X^2Z^4, A'_{31} = \sqrt{\tilde{p}'_{31}}X^2Z^5, \\
A'_{32} &= \sqrt{\tilde{p}'_{32}}X^2Z^6, A'_{33} = \sqrt{\tilde{p}'_{33}}X^2Z^7, A'_{34} = \sqrt{\tilde{p}'_{34}}Z^1X^3, A'_{35} = \sqrt{\tilde{p}'_{35}}Z^2X^3, A'_{36} = \sqrt{\tilde{p}'_{36}}X^3Z^4, \\
A'_{37} &= \sqrt{\tilde{p}'_{37}}X^3Z^5, A'_{38} = \sqrt{\tilde{p}'_{38}}X^3Z^6, A'_{39} = \sqrt{\tilde{p}'_{39}}X^3Z^7, A'_{40} = \sqrt{\tilde{p}'_{40}}Z^1X^4, A'_{41} = \sqrt{\tilde{p}'_{41}}Z^2X^4, \\
A'_{42} &= \sqrt{\tilde{p}'_{42}}Z^3X^4, A'_{43} = \sqrt{\tilde{p}'_{43}}X^4Z^5, A'_{44} = \sqrt{\tilde{p}'_{44}}X^4Z^6, A'_{45} = \sqrt{\tilde{p}'_{45}}X^4Z^7, A'_{46} = \sqrt{\tilde{p}'_{46}}Z^1X^5, \tag{B3}
\end{aligned}$$

and,

$$\begin{aligned}
A'_{47} &= \sqrt{\tilde{p}'_{47}}Z^2X^5, A'_{48} = \sqrt{\tilde{p}'_{48}}Z^3X^5, A'_{49} = \sqrt{\tilde{p}'_{49}}Z^4X^5, A'_{50} = \sqrt{\tilde{p}'_{50}}X^5Z^6, A'_{51} = \sqrt{\tilde{p}'_{51}}X^5Z^7, \\
A'_{52} &= \sqrt{\tilde{p}'_{52}}Z^1X^6, A'_{53} = \sqrt{\tilde{p}'_{53}}Z^2X^6, A'_{54} = \sqrt{\tilde{p}'_{54}}Z^3X^6, A'_{55} = \sqrt{\tilde{p}'_{55}}Z^4X^6, A'_{56} = \sqrt{\tilde{p}'_{56}}Z^5X^6, \\
A'_{57} &= \sqrt{\tilde{p}'_{57}}X^6Z^7, A'_{58} = \sqrt{\tilde{p}'_{58}}Z^1X^7, A'_{59} = \sqrt{\tilde{p}'_{59}}Z^2X^7, A'_{60} = \sqrt{\tilde{p}'_{60}}Z^3X^7, A'_{61} = \sqrt{\tilde{p}'_{61}}Z^4X^7, \\
A'_{62} &= \sqrt{\tilde{p}'_{62}}Z^5X^7, A'_{63} = \sqrt{\tilde{p}'_{63}}Z^6X^7. \tag{B4}
\end{aligned}$$

Detectable Errors (Set-1). For the sake of completeness, we show in an explicit way that these 64 errors are detectable. Considering $k \in \{0, 1, \dots, 21\}$, the error syndrome of weight-0 and weight-1 error operators is given by,

$$\begin{aligned}
S(I) &= 000000, S(X^1) = 111000, S(X^2) = 110000, S(X^3) = 101000, S(X^4) = 100000, \\
S(X^5) &= 011000, S(X^6) = 010000, S(X^7) = 001000, S(Y^1) = 111111, S(Y^2) = 110110, \\
S(Y^3) &= 101101, S(Y^4) = 100100, S(Y^5) = 011011, S(Y^6) = 010010, S(Y^7) = 001001, \\
S(Z^1) &= 000111, S(Z^2) = 000110, S(Z^3) = 000101, S(Z^4) = 000100, S(Z^5) = 000011, \\
S(Z^6) &= 000010, S(Z^7) = 000001. \tag{B5}
\end{aligned}$$

Instead, for $k \in \{22, \dots, 63\}$ the error syndrome of weight-2 error operators is given by,

$$\begin{aligned}
S(X^1Z^2) &= 111110, S(X^1Z^3) = 111101, S(X^1Z^4) = 111100, S(X^1Z^5) = 111011, S(X^1Z^6) = 111010, \\
S(X^1Z^7) &= 111001, S(Z^1X^2) = 110111, S(X^2Z^3) = 110101, S(X^2Z^4) = 110100, S(X^2Z^5) = 110011, \\
S(X^2Z^6) &= 110010, S(X^2Z^7) = 110001, S(Z^1X^3) = 101111, S(Z^2X^3) = 101110, S(X^3Z^4) = 101100, \\
S(X^3Z^5) &= 101011, S(X^3Z^6) = 101010, S(X^3Z^7) = 101001, S(Z^1X^4) = 100111, S(Z^2X^4) = 100110, \\
S(Z^3X^4) &= 100101, S(X^4Z^5) = 100011, S(X^4Z^6) = 100010, S(X^4Z^7) = 100001, S(Z^1X^5) = 011111, \tag{B6}
\end{aligned}$$

and,

$$\begin{aligned}
S(Z^2 X^5) &= 011110, S(Z^3 X^5) = 011101, S(Z^4 X^5) = 011100, S(X^5 Z^6) = 011010, S(X^5 Z^7) = 011001, \\
S(Z^1 X^6) &= 010111, S(Z^2 X^6) = 010110, S(Z^3 X^6) = 010101, S(Z^4 X^6) = 010100, S(Z^5 X^6) = 010011, \\
S(X^6 Z^7) &= 010001, S(Z^1 X^7) = 001111, S(Z^2 X^7) = 001110, S(Z^3 X^7) = 001101, S(Z^4 X^7) = 001100, \\
S(Z^5 X^7) &= 001011, S(Z^6 X^7) = 001010.
\end{aligned} \tag{B7}$$

Since these errors have non-vanishing error syndromes, they are detectable. As a side remark, we point out that following the above-mentioned line of reasoning, it can be shown that $S(A_l^\dagger A_k') \neq 0$, with $l, k \in \{0, 1, \dots, 63\}$.

Entanglement Fidelity (Set-1). The explicit expression for $\mathcal{F}_{\text{Set-1}}^{[[7,1,3]]}(\mu, p)$ in (67) is given by,

$$\begin{aligned}
\mathcal{F}_{\text{Set-1}}^{[[7,1,3]]}(\mu, p) &= \mu^6 \left(\frac{4}{3}p^7 - p^6 - \frac{5}{3}p^5 + \frac{4}{3}p^4 \right) + \mu^5 \left(-8p^7 + \frac{50}{3}p^6 - \frac{22}{3}p^5 - 4p^4 + \frac{8}{3}p^3 \right) + \\
&\mu^4 \left(20p^7 - \frac{205}{3}p^6 + \frac{250}{3}p^5 - 41p^4 + \frac{14}{3}p^3 + \frac{4}{3}p^2 \right) + \\
&\mu^3 \left(-\frac{80}{3}p^7 + \frac{380}{3}p^6 - \frac{680}{3}p^5 + 192p^4 - \frac{232}{3}p^3 + 12p^2 \right) + \\
&\mu^2 \left(20p^7 - \frac{365}{3}p^6 + \frac{835}{3}p^5 - 310p^4 + \frac{530}{3}p^3 - \frac{145}{3}p^2 + 5p \right) + \\
&\mu \left(-8p^7 + \frac{178}{3}p^6 - \frac{490}{3}p^5 + 220p^4 - \frac{460}{3}p^3 + \frac{154}{3}p^2 - 6p \right) + \\
&\left(\frac{4}{3}p^7 - \frac{35}{3}p^6 + \frac{112}{3}p^5 - \frac{175}{3}p^4 + \frac{140}{3}p^3 - \frac{49}{3}p^2 + 1 \right).
\end{aligned} \tag{B8}$$

Error Operators (Set-2). The sets of weight-0 and weight-1 correctable errors are given in (B1) and (B2), respectively. The chosen set of correctable weight-2 error operators is,

$$\begin{aligned}
A''_{22} &= \sqrt{\tilde{p}''_{22}} Z^1 Z^2, A''_{23} = \sqrt{\tilde{p}''_{23}} Z^1 Z^3, A''_{24} = \sqrt{\tilde{p}''_{24}} Z^1 Z^4, A''_{25} = \sqrt{\tilde{p}''_{25}} Z^1 Z^5, A''_{26} = \sqrt{\tilde{p}''_{26}} Z^1 Z^6, \\
A''_{27} &= \sqrt{\tilde{p}''_{27}} Z^1 Z^7, A''_{28} = \sqrt{\tilde{p}''_{28}} Z^2 Z^3, A''_{29} = \sqrt{\tilde{p}''_{29}} Z^2 Z^4, A''_{30} = \sqrt{\tilde{p}''_{30}} Z^2 Z^5, A''_{31} = \sqrt{\tilde{p}''_{31}} Z^2 Z^6, \\
A''_{32} &= \sqrt{\tilde{p}''_{32}} Z^2 Z^7, A''_{33} = \sqrt{\tilde{p}''_{33}} Z^3 Z^4, A''_{34} = \sqrt{\tilde{p}''_{34}} Z^3 Z^5, A''_{35} = \sqrt{\tilde{p}''_{35}} Z^3 Z^6, A''_{36} = \sqrt{\tilde{p}''_{36}} Z^3 Z^7, \\
A''_{37} &= \sqrt{\tilde{p}''_{37}} Z^4 Z^5, A''_{38} = \sqrt{\tilde{p}''_{38}} Z^4 Z^6, A''_{39} = \sqrt{\tilde{p}''_{39}} Z^4 Z^7, A''_{40} = \sqrt{\tilde{p}''_{40}} Z^5 Z^6, A''_{41} = \sqrt{\tilde{p}''_{41}} Z^5 Z^7, \\
A''_{42} &= \sqrt{\tilde{p}''_{42}} Z^6 Z^7,
\end{aligned} \tag{B9}$$

and,

$$\begin{aligned}
A''_{43} &= \sqrt{\tilde{p}''_{43}} Z^1 X^2, A''_{44} = \sqrt{\tilde{p}''_{44}} Z^1 X^3, A''_{45} = \sqrt{\tilde{p}''_{45}} Z^1 X^4, A''_{46} = \sqrt{\tilde{p}''_{46}} Z^1 X^5, \\
A''_{47} &= \sqrt{\tilde{p}''_{47}} Z^1 X^6, A''_{48} = \sqrt{\tilde{p}''_{48}} Z^1 X^7, A''_{49} = \sqrt{\tilde{p}''_{49}} Z^2 X^3, A''_{50} = \sqrt{\tilde{p}''_{50}} Z^2 X^4, A''_{51} = \sqrt{\tilde{p}''_{51}} Z^2 X^5, \\
A''_{52} &= \sqrt{\tilde{p}''_{52}} Z^2 X^6, A''_{53} = \sqrt{\tilde{p}''_{53}} Z^2 X^7, A''_{54} = \sqrt{\tilde{p}''_{54}} Z^3 X^4, A''_{55} = \sqrt{\tilde{p}''_{55}} Z^3 X^5, A''_{56} = \sqrt{\tilde{p}''_{56}} Z^3 X^6, \\
A''_{57} &= \sqrt{\tilde{p}''_{57}} Z^3 X^7, A''_{58} = \sqrt{\tilde{p}''_{58}} Z^4 X^5, A''_{59} = \sqrt{\tilde{p}''_{59}} Z^4 X^6, A''_{60} = \sqrt{\tilde{p}''_{60}} Z^4 X^7, A''_{61} = \sqrt{\tilde{p}''_{61}} Z^5 X^6, \\
A''_{62} &= \sqrt{\tilde{p}''_{62}} Z^5 X^7, A''_{63} = \sqrt{\tilde{p}''_{63}} Z^6 X^7.
\end{aligned} \tag{B10}$$

Entanglement Fidelity (Set-2). The explicit expression for $\mathcal{F}_{\text{Set-2}}^{[[7,1,3]]}(\mu, p)$ in (71) is given by,

$$\begin{aligned}
\mathcal{F}_{\text{Set-2}}^{[[7,1,3]]}(\mu, p) &= \mu^6 \left(\frac{4}{3} p^7 + p^6 - 5p^5 + \frac{8}{3} p^4 \right) + \mu^5 \left(-8p^7 + \frac{20}{3} p^6 + 16p^5 - \frac{64}{3} p^4 + \frac{20}{3} p^3 \right) + \\
&\quad \mu^4 \left(20p^7 - \frac{145}{3} p^6 + \frac{70}{3} p^5 + 23p^4 - \frac{70}{3} p^3 + \frac{16}{3} p^2 \right) + \\
&\quad \mu^3 \left(-\frac{80}{3} p^7 + \frac{320}{3} p^6 - \frac{460}{3} p^5 + \frac{272}{3} p^4 - \frac{40}{3} p^3 - \frac{16}{3} p^2 + \frac{4}{3} p \right) + \\
&\quad \mu^2 \left(20p^7 - \frac{335}{3} p^6 + 235p^5 - \frac{710}{3} p^4 + \frac{350}{3} p^3 - 25p^2 + \frac{5}{3} p \right) + \\
&\quad \mu \left(-8p^7 + \frac{172}{3} p^6 - \frac{460}{3} p^5 + 200p^4 - \frac{400}{3} p^3 + \frac{124}{3} p^2 - 4p \right) + \\
&\quad \left(\frac{4}{3} p^7 - \frac{35}{3} p^6 + \frac{112}{3} p^5 - \frac{175}{3} p^4 + \frac{140}{3} p^3 - \frac{49}{3} p^2 + 1 \right).
\end{aligned} \tag{B11}$$

Appendix C: Asymmetries and Correlations

Entanglement Fidelity. Substituting (80) in (79) the explicit expression for $\mathcal{F}_{\text{asymmetric}}^{[[7,1,3]]}(\mu, p)$ becomes,

$$\mathcal{F}_{\text{asymmetric}}^{[[7,1,3]]}(\mu, p) = \mathcal{A}_6(\mu, p) + \mathcal{A}_5(\mu, p) + \mathcal{A}_4(\mu, p) + \mathcal{A}_3(\mu, p) + \mathcal{A}_2(\mu, p) + \mathcal{A}_1(\mu, p) + \mathcal{A}_0(\mu, p). \tag{C1}$$

The quantities $\mathcal{A}_6(\mu, p)$, $\mathcal{A}_5(\mu, p)$, $\mathcal{A}_4(\mu, p)$ and $\mathcal{A}_3(\mu, p)$ are given by,

$$\begin{aligned}
\mathcal{A}_6(\mu, p) &= \mu^6 \left[(6p^7 - 11p^6 + 5p^5) + \alpha_Z (6p^6 - 10p^5 + 4p^4) + (\alpha_Z^2 + \alpha_X \alpha_Z) (-21p^7 + 45p^6 - 30p^5 + 6p^4) \right], \\
\mathcal{A}_5(\mu, p) &= \mu^5 \left[\begin{aligned} &(-36p^7 + 90p^6 - 74p^5 + 20p^4) + \alpha_Z (-30p^6 + 70p^5 - 52p^4 + 12p^3) + \\ &+ (\alpha_Z^2 + \alpha_X \alpha_Z) (126p^7 - 330p^6 + 300p^5 - 108p^4 + 12p^3) \end{aligned} \right], \\
\mathcal{A}_4(\mu, p) &= \mu^4 \left[\begin{aligned} &(90p^7 - 285p^6 + 330p^5 - 165p^4 + 30p^3) + \alpha_Z (60p^6 - 180p^5 + 192p^4 - 84p^3 + 12p^2) + \\ &+ (\alpha_Z^2 + \alpha_X \alpha_Z) (-315p^7 + 975p^6 - 1110p^5 + 558p^4 - 114p^3 + 6p^2) \end{aligned} \right], \\
\mathcal{A}_3(\mu, p) &= \mu^3 \left[\begin{aligned} &(-120p^7 + 460p^6 - 680p^5 + 480p^4 - 160p^3 + 20p^2) + \\ &+ \alpha_Z (-60p^6 + 220p^5 - 304p^4 + 192p^3 - 52p^2 + 4p) + \\ &+ (\alpha_Z^2 + \alpha_X \alpha_Z) (420p^7 - 1500p^6 + 2040p^5 - 1296p^4 + 372p^3 - 36p^2) \end{aligned} \right], \tag{C2}
\end{aligned}$$

while $\mathcal{A}_2(\mu, p)$, $\mathcal{A}_1(\mu, p)$ and $\mathcal{A}_0(\mu, p)$ are,

$$\begin{aligned}
\mathcal{A}_2(\mu, p) &= \mu^2 \left[\begin{aligned} &(90p^7 - 405p^6 + 725p^5 - 650p^4 + 300p^3 - 65p^2 + 5p) + \\ &+ \alpha_Z (30p^6 - 130p^5 + 220p^4 - 180p^3 + 70p^2 - 10p) + \\ &+ (\alpha_Z^2 + \alpha_X \alpha_Z) (-315p^7 + 1275p^6 - 2010p^5 + 1530p^4 - 555p^3 + 75p^2) \end{aligned} \right], \\
\mathcal{A}_1(\mu, p) &= \mu \left[\begin{aligned} &(-36p^7 + 186p^6 - 390p^5 + 420p^4 - 240p^3 + 66p^2 - 6p) + \\ &+ \alpha_Z (-6p^6 + 30p^5 - 60p^4 + 60p^3 - 30p^2 + 6p) + \\ &+ (\alpha_Z^2 + \alpha_X \alpha_Z) (126p^7 - 570p^6 + 1020p^5 - 900p^4 + 390p^3 - 66p^2) \end{aligned} \right], \\
\mathcal{A}_0(\mu, p) &= (1-p)^7 + 7p(1-p)^6 + 21p^2(1-p)^5 [\alpha_Z^2 + \alpha_X \alpha_Z]. \tag{C3}
\end{aligned}$$

-
- [1] D. Gottesman, "An Introduction to Quantum Error Correction and Fault-Tolerant Quantum Computation", arXiv:quant-ph/0904.2557 (2009).
[2] E. Knill and R. Laflamme, "Theory of quantum error-correcting codes", Phys. Rev. **A55**, 900 (1997).
[3] A. R. Calderbank et al., "Quantum Error Correction and Orthogonal Geometry", Phys. Rev. Lett. **78**, 405 (1997).
[4] A. Garg, "Decoherence in Ion Trap Quantum Computers", Phys. Rev. Lett. **77**, 964 (1996).
[5] D. Loss and D. P. Di Vincenzo, "Quantum computation with quantum dots", Phys. Rev. **A57**, 120 (1998).
[6] W. Y. Hwang et al., "Correlated errors in quantum-error corrections", Phys. Rev. **A63**, 022303 (2001).
[7] J. P. Clemens et al., "Quantum error correction against correlated noise", Phys. Rev. **A69**, 062313 (2004).
[8] R. Klesse and S. Frank, "Quantum Error Correction in Spatially Correlated Quantum Noise", Phys. Rev. Lett. **95**, 230503 (2005).
[9] A. Shabani, "Correlated errors can lead to better performance of quantum codes", Phys. Rev. **A77**, 022323 (2008).
[10] A. D'Arrigo et al., "Memory effects in a Markovian chain dephasing channel", Int. J. Quantum Inf. **6**, 651 (2008).
[11] C. Cafaro and S. Mancini, "Repetition Versus Noiseless Quantum Codes For Correlated Errors", Phys. Lett. **A374**, 2688 (2010).
[12] O. Astafiev et al., "Quantum Noise in the Josephson Charge Qubit", Phys. Rev. Lett. **93**, 267007 (2004).
[13] L. Ioffe and M. Mezard, "Asymmetric quantum error correcting codes", Phys. Rev. **A75**, 032345 (2007).

- [14] Z. W. E. Evans et al. , "Error Correction Optimisation in The Presence of X/Z Asymmetry", arXiv:quant-ph/0709.3875 (2007).
- [15] A. M. Stephens et al. , "Asymmetric quantum error correction via code conversion", Phys. Rev. **A77**, 062335 (2008).
- [16] P. K. Sarvepalli et al., "Asymmetric Quantum LDPC Codes", arXiv:quant-ph/0804.4316 (2008).
- [17] S. A. Aly, "Asymmetric and Symmetric Subsystem BCH Codes and Beyond", arXiv:quant-ph/0803.0764 (2008).
- [18] D. Gottesman, "Stabilizer Codes and Quantum Error Correction", PhD Thesis, California Institute of Technology, Pasadena, CA (1997).
- [19] B. Schumacher, "Sending entanglement through noisy quantum channels", Phys. Rev. **A54**, 2615 (1996).
- [20] R. Laflamme et al., "Perfect quantum error correcting code", Phys. Rev. Lett. **77**, 198 (1996).
- [21] M. A. Nielsen and I. L. Chuang, "Quantum Computation and Information", Cambridge University Press (2000).
- [22] R. A. Calderbank et al., "Quantum error correction via codes over $GF(4)$ ", IEEE Trans. Inf. Theor. **44**, 1369 (1998).
- [23] E. Knill et al., "Introduction to Quantum Error Correction", arXiv:quant-ph/020717 (2002).
- [24] P. Kaye, R. Laflamme and M. Mosca, "An Introduction to Quantum Computing", Oxford University Press (2007).
- [25] M. A. Nielsen, "The entanglement fidelity and quantum error correction", arXiv: quant-ph/9606012 (1996).
- [26] F. Gaitan, "Quantum Error Correction and Fault Tolerant Quantum Computing", CRC Press (2008).
- [27] A. R. Calderbank and P. W. Shor, "Good quantum error correcting codes exist", Phys. Rev. **A54**, 1098 (1996).
- [28] A. M. Steane, "Multiple-particle interference and quantum error correction", Proc. R. Soc. Lond. **A452**, 2551 (1996).
- [29] D. Zaslavsky, "Fault Tolerant Quantum Computation with Asymmetric Error Probabilities", BS Thesis, Princeton University, Princeton, NJ (2008).
- [30] E. Knill, "Quantum computing with realistically noisy devices", Nature **434**, 39 (2005).